Research paper

The link between tectonics and sedimentation in asymmetric extensional basins: Inferences from the study of the Sarajevo-Zenica Basin

N. Andrić [a, b, *], K. Sant [a], L. Matenco [a], O. Mandic [c], B. Tomljenović [d], D. Pavelić [d], H. Hrvatović [e], V. Demir [e], J. Ooms [a]

[a] Utrecht University, Faculty of Geosciences, Utrecht, The Netherlands
[b] University of Belgrade, Faculty of Mining and Geology, Belgrade, Serbia
[c] Naturhistorisches Museum Wien, Geologisch-Paläontologische Abteilung, Burgring 7, A-1010 Wien, Austria
[d] University of Zagreb, Faculty of Mining, Geology & Petroleum Engineering, Zagreb, Croatia
[e] Federal Institute for Geology - Sarajevo, Ustanička 11, 71210 Ilidža, Bosnia and Herzegovina

ARTICLE INFO

ABSTRACT

The coupled tectonic and depositional history of extensional basins is usually described in terms of stratigraphic sequences linked with the activity of normal faults. This depositional-kinematic interplay is less understood in basins bounded by major extensional detachments or normal fault systems associated with significant exhumation of footwalls. Of particular interest is the link between tectonics and sedimentation during the migration of normal faulting in time and space across the basin. One area where such coupled depositional-kinematic history can be optimally studied is the Late Oligocene - Miocene Sarajevo-Zenica Basin, located in the Dinarides Mountains of Bosnia and Herzegovina. This intramontane basin recorded Oligocene − Pliocene sedimentation in an endemic and isolated lake environment. We use field kinematic and sedimentological mapping in outcrops correlated with existing local and regional studies to derive a high-resolution evolutionary model of the basin. The novel results demonstrate a close correlation between moments of normal faulting and high-order sedimentological cycles, while the overall extensional basin was filled by a largely uni-directional sediment supply from the neighbouring mountain chain. The migration in time and space of listric NE-dipping normal faults was associated with a gradual shift of the sedimentological environment. Transgressive-regressive cycles reflect sequential displacements on normal faults and their footwall exhumation, defining a new sedimentological model for such basins. This Early - Middle Miocene extension affected the central part of the Dinarides and was associated with the larger opening of the neighbouring Pannonian Basin. The extension was preceded and followed by two phases of contraction. The Oligocene - Early Miocene thrusting took place during the final stages of the Dinarides collision, while the post-Middle Miocene contraction is correlated with the regional indentation of the Adriatic continental unit. This latter phase inverted the extensional basin by reactivating the inherited basal listric detachment.

© 2017 Elsevier Ltd. All rights reserved.

1. Introduction

Depositional geometries are controlled by the balance between sediment supply and accommodation space, which is enhanced in tectonically active basins (e.g., Schlager, 1993; Miall and Miall, 2001; Cloetingh and Haq, 2015; Balázs et al., 2016). The relationship between tectonic and sedimentation has been extensively studied in rift systems by the means of seismostratigraphic interpretations correlated with wells and/or observations in outcrops, either in extensional structures buried beneath passive continental margins, or in similar basins exposed onshore (e.g., van Wagoner et al., 1990; Nottvedt et al., 1995; Hinsken et al., 2007; Martins-Neto and Catuneanu, 2010). These studies have demonstrated that moments of deformation are associated with a depositional cyclicity. The creation of accommodation space is enhanced

* Corresponding author. Utrecht University, Department of Earth Sciences, PO Box: 80021, 3508TA Utrecht, The Netherlands.
E-mail address: n.andric@uu.nl (N. Andrić).

in the hanging-wall of normal faults, while footwall erosion is a good indicator for regressive patterns. Such relationships are less obvious in the case of asymmetric extensional basins, i.e. basins where sedimentation is controlled by either a major extensional detachment, or by a system of uni-directional dipping listric normal faults that are connected at depth to one major shear zone, as observed, for instance, in extensional break-away or supra-detachment basins (e.g., Wernicke, 1992; Friedmann and Burbank, 1995; Ziegler and Cloetingh, 2004; Rosenbaum et al., 2005; Tugend et al., 2014). Asymmetries are favoured when pre-existing crustal rheological contrasts are inherited, such as thrusts, orogenic nappe stacks or suture zones, frequently observed in extensional back-arc basins during the evolution of detachment faults that exhume rocks previously buried at high depths (e.g., Bertotti et al., 2000; Brun and Faccenna, 2008; van Wijk et al., 2008). Numerous examples are observed during the Paleogene - Miocene evolution of orogens in the Mediterranean region, when slab rollback was associated with back-arc extension and the formation of a large number of core-complexes and extensional basins bounded by detachments or low-angle normal faults (Jolivet and Faccenna, 2000; Faccenna et al., 2004; Jolivet and Brun, 2010). In such basins, sedimentation is not only controlled by the position of the central subsiding area, but also by the gradual migration in space and time of normal faulting combined with enhanced exhumation of footwalls (Lister and Davis, 1989; Martín-Barajas et al., 2001; Bargnesi et al., 2013).

One area where the formation of asymmetric extensional basins was controlled by detachments reactivating pre-existing thrusts is the Dinarides - Pannonian system (Fig. 1a, b, e.g., Balázs et al., 2016). For instance, the inherited Cretaceous suture zone between Adria and Europe (i.e. the Sava Zone) was reactivated by extension along its entire strike (e.g., Ustaszewski et al., 2010; van Gelder et al., 2015). This extension created (Oligocene-) Miocene extensional basins that are either parts of the larger Pannonian Basin system (e.g., Tari et al., 1992; Horváth et al., 2015), or evolved in an endemic and/or geographically isolated environment within the Dinaride Lake System (Harzhauser and Mandic, 2008). In this latter system, the largest basin is Sarajevo-Zenica that formed on the northern flank of the Mid-Bosnian Schist Mountains, near the inherited nappe contact between the Pre-Karst and East Bosnian - Durmitor units (Fig. 1b). The basin was filled with alluvial-fluvial and lacustrine sediments deposited during Oligocene - Pliocene times and has a highly asymmetric stratigraphic geometry controlled by a large fault, or a system of faults, located at its SW margin (Fig. 1b, the Busovača Fault of Hrvatović, 2006). Interesting is the isolated nature of the basin, which evolved entirely in an isolated and endemic environment during its entire existence (Milojević, 1964). This allows a direct correlation between erosion in the neighbouring source area and deposition inside the basin, although lake-level variations, controlled by the local balance between precipitation and evapo-transpiration, are rather frequent in such systems (e.g., Garcia-Castellanos et al., 2003; Leever et al., 2011).

The kinematic and sedimentological field observations performed on existing outcrops were correlated with previous local and regional studies (e.g., Hrvatović, 2006 and references therein) in order to derive a high-resolution evolutionary model of the Sarajevo-Zenica Basin. These observations were taken along a number of transects and isolated outcrops that were correlated based on field mapping, synchronicity of faulting events and associated sedimentary wedges in the basin and, whenever available, existing biostratigraphic information. Field observations were used to separate kinematic phases of deformation and individual episodes of faulting. This kinematics was coupled with

sedimentological observations for the period of extensional deformation by following a standard approach including the definition of facies units, facies associations, sedimentological environment and systems tracts. Systems tracts are fault-controlled and were used to correlate the kinematic episodes and quantify the evolution of accommodation space in the basin. The ultimate target is to define a new tectonic model of coupled tectonic and depositional evolution for asymmetric extensional basins. This model is still specific to the Sarajevo-Zenica Basin, but the principles of its construction are generic and can be applied to similar basins worldwide. Furthermore, the kinematic model of basin evolution has significant novel inferences for understanding the tectonics of the Dinarides.

2. The Sarajevo-Zenica Basin in the context of the larger Dinarides evolution

The Dinarides formed in response to the Triassic opening of the Neotethys Ocean between Europe- and Adriatic-derived continental units and its subsequent closure that started during Middle - Late Jurassic times (Fig. 1, Pamić, 2002; Schmid et al., 2008; Handy et al., 2015). The internal parts of Dinarides were tectonically overlain by ophiolites and genetically associated ophiolitic melanges during the Late Jurassic - earliest Cretaceous obduction stages (e.g., Dimitrijević and Dimitrijević, 1991; Đerić et al., 2007; Schmid et al., 2008; Robertson, 2011). The orogen was subsequently built-up during subsequent Cretaceous - Eocene shortening events that created an overall nappe stack where deformation generally migrated in time towards the Adriatic foreland (Fig. 1, e.g., Dimitrijević, 1997; Schmid et al., 2008). The contraction is still active at present (e.g., Bennett et al., 2008; Herak et al., 2009). The nappes are made up by a Paleozoic basement affected by various degrees of Variscan deformation and metamorphism that was unconformably covered by a dominantly carbonatic Permian - Eocene succession (e.g., Đoković, 1985; Korbar, 2009).

2.1. Available constraints from the tectonic and sedimentary evolution

The Late Jurassic - Eocene contraction was locally associated with the deposition of syn-contractional trench turbidites (i.e. flysch deposits). Elongated areas of such highly-deformed sediments follow thrust contacts along the Dinarides strike (e.g., Dimitrijević and Dimitrijević, 1987). Among them, the Bosnian Flysch recorded a Late Jurassic - latest Cretaceous deposition of mixed carbonate and siliciclastic sediments (e.g., Aubouin et al., 1970; Rampnoux, 1970; Mikes et al., 2008b), which overlies the upper and internal parts of the Pre-Karst unit (Fig. 1). Thrusting over the Bosnian Flysch separates the dominant Triassic - Lower Eocene shallow-water Adriatic carbonate platform deposition observed in more external Dinarides units (Dalmatian, Budva - Cukali, High Karst, and Pre-Karst units) from more internal units carrying obducted ophiolites in an upper structural position (East Bosnian - Durmitor, Drina - Ivanjica and Jadar — Kopaonik units) and recorded a late Middle Triassic - Early Jurassic gradual deepening of their carbonatic facies (Fig. 1, Dimitrijević, 1997; Pamić, 2002; Schmid et al., 2008). The Bosnian Flysch was significantly deformed in successive phases of thrusting and is divided into two units separated by local unconformities: an older and more internal Late Jurassic - Berriasian Vranduk Flysch, and a younger and more external Turronian - Senonian Ugar - Durmitor Flysch unit that extends ESE-wards until the junction with the Albanides
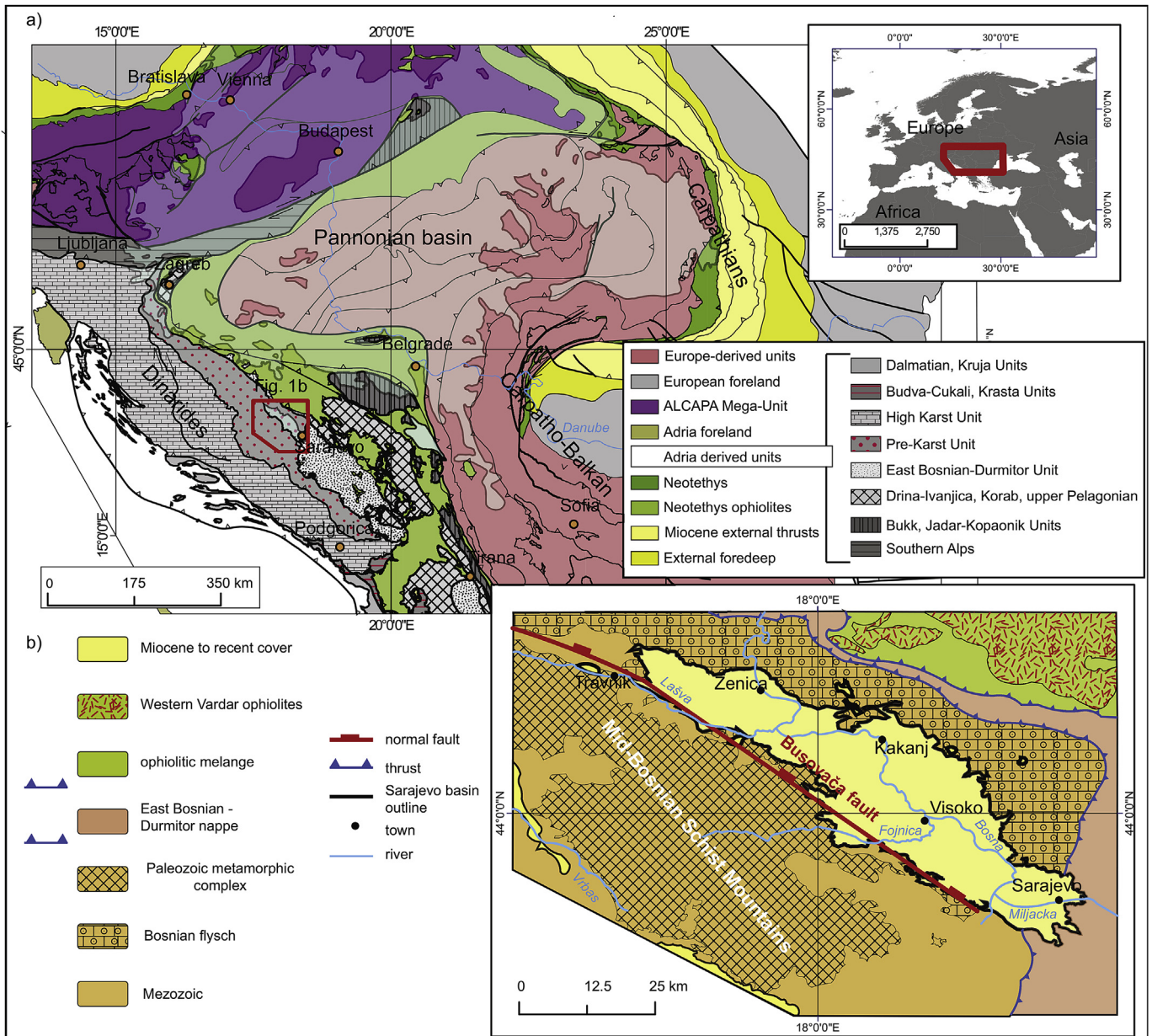
Fig. 1. a) Tectonic map of the Alps - Carpathians - Dinarides system (simplified after Schmid et al., 2008). White and transparent white polygons show the locations of Miocene basins, such as the Pannonian. Red polygon outlines the location of the Sarajevo–Zenica Basin. Inset represents the location of the map. b) Simplified tectonic map of the Central Dinarides with the outline of the Sarajevo-Zenica Basin (after Jovanović et al., 1971; Sofilj and Živanović, 1971; Olujić et al., 1978; Živanović et al., 1967). (For interpretation of the references to colour in this figure legend, the reader is referred to the web version of this article.)

(Rampnoux, 1970; Dimitrijević, 1997; Hrvatović and Pamić, 2005).

The internal part of the Dinarides was affected by significant extension, which is generally related with the back-arc opening of the Pannonian Basin starting at ~20 Ma, driven by the rapid Miocene retreat of the Carpathian subduction zone (Fodor et al., 1999; Horváth et al., 2015 and references therein). The extension in the north − eastern Dinarides started during the Late Oligocene, migrated in space and time and recorded peak moments during the Middle Miocene (~14–15 Ma) (de Leeuw et al., 2012; Matenco and Radivojević, 2012). Large-scale extensional detachments inverted the Adria - Europe suture zone (i.e. the Sava zone), as well as various thrust contacts in the Dinarides and thus exhumed parts of tectonic units previously deeply buried in their footwalls

(Ustaszewski et al., 2010; Schefer et al., 2011; Stojadinović et al., 2013; Toljić et al., 2013; van Gelder et al., 2015). These detachments are locally observed along the strike of the Dinarides near their NE margin and are also buried beneath the Miocene sediments of the Pannonian Basin (Matenco and Radivojević, 2012). The systems of low-angle normal faults, their exhumed footwalls and hanging-wall basins have similar structural geometries and have also comparable mechanisms with the Miocene extension affecting the transition between the Alps and the Pannonian Basin (Ratschbacher et al., 1991; Tari et al., 1992; Cao et al., 2013).

The contraction near the frontal part of the Dinarides and the coeval extension in more internal areas created the accommodation space for the formation of many Miocene lakes, which recorded

shallow water lacustrine to continental alluvial deposition in a mostly endemic and/or geographically isolated environment (Krstić et al., 2003; Harzhauser and Mandic, 2008; de Leeuw et al., 2012). The endemic and often isolated nature of these basins provided important constraints for the palaeoenvironmental and palaeobiogeographic evolution of the Dinarides region (Jiménez-Moreno et al., 2009; de Leeuw et al., 2010; Mandic et al., 2011). Some basins formed and evolved separately as individual and isolated depocentres (the Dinaride Lake System of de Leeuw et al., 2012), while others are interpreted as remnants of a single lake (Lake Serbia, Krstić et al., 2003). While the isolation of northern basins ceased during a Middle Miocene marine transgression, the deposition in smaller basins in the External Dinarides apparently stopped at the same time (de Leeuw et al., 2012; Mandic et al., 2012). The Neogene deposits of the Dinarides have been deformed by contraction during the Adria indentation starting during latest Miocene times (e.g., Ustaszewski et al., 2014). Although a number of tectonic hypotheses have been suggested for the formation of the entire lake system, such as transtensional opening due to the movements along the Peri-Adriatic lineament (Hrvatović, 2006) or wedge-top basins (Korbar, 2009), the detailed tectonic and sedimentary evolution of most of these Oligocene - Miocene basins is largely unknown (Mikes et al., 2008a).

2.2. The geological evolution of the Sarajevo - Zenica Basin

The Sarajevo-Zenica Basin (Fig. 1) is the largest in the Dinaride Lake System and has received little attention in published geological studies. It overlies a paleorelief formed during successive Late Jurassic - Cretaceous thrusting events at the contact between the East Bosnian - Durmitor and Pre-Karst units, the latter including a thick sequence of highly deformed Bosnian Flysch that outcrops dominantly along the NE basin flank (Fig. 1b, e.g., Hrvatović, 2006; Schmid et al., 2008). The strike of this contact swings in map view from NW-SE in Montenegro and eastern Bosnia and Herzegovina to N-S and further back to NW-SE westwards, coinciding with a significant reduction in the exposed width of the East Bosnian - Durmitor unit (Fig. 1, the Sarajevo sigmoid of Dimitrijević, 1997). Outside the Bosnian Flysch sediments described above, the SW basin margin is made up by the Paleozoic metamorphic complex of Mid-Bosnian Schist Mountains overlain by an undifferentiated Mesozoic cover (Fig. 1b). The Mid-Bosnian Schist Mountains include Variscan metasediments and meta-volcanics together with limestones, dolomite and Permian post-Varisan continental sediments (e.g., Hrvatović, 2006). The Mesozoic cover contains clastics and carbonate sediments deposited on the passive continental margin during Triassic times together with Middle Triassic rifting magmatics (diabases, diorites, gabbros, syenites, spilites and quartitic andesites).

Existing biostratigraphic constraints of the Sarajevo-Zenica basin were derived from regional geological correlation of pollen and mollusk records (e.g. Hrvatović, 2006). This stratigraphic scheme is less accurate (see details in de Leeuw et al., 2012) and may be further updated through independent geochronological methods.

Starting with Late Oligocene times, the evolution of the Sarajevo-Zenica Basin is thought to be controlled by the large NW-SE striking Busovača Fault recognized near the SW margin from surface mapping, well data and geophysical interpretations (Fig. 1, Hrvatović, 2006). Along the northern margin of the basin, Upper Oligocene - Miocene sediments were deposited unconformably over the Bosnian Flysch sediments (Hrvatović, 2006). South of the Busovača Fault, exhumed areas of the Mid-Bosnian Schist Mountains expose their Paleozoic core made up by sediments affected by various degrees of Caledonian, Variscan and Cretaceous metamorphism that are covered along their strike by Mesozoic
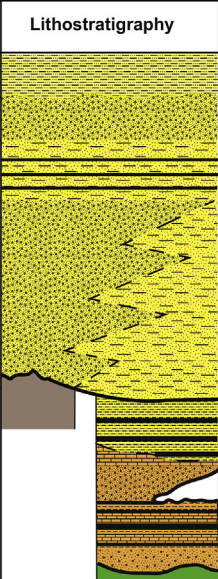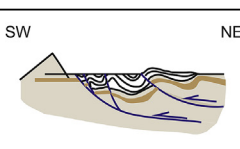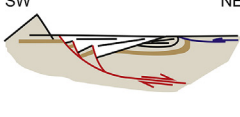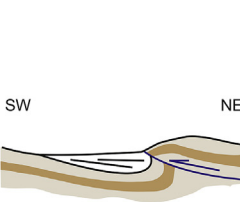
sediments of the Adriatic carbonate platform (Pamić et al., 2004; Hrvatović and Pamić, 2005). Low temperature thermochronological dating of the exhumation that have inferred ages ~42–27 Ma and 29–24 Ma for zircon fission tracks and U-Th/He, and ~7–5 Ma for apatite U-Th/He (Casale, 2012; Hrvatović et al., 2015). These ages have been interpreted to reflect the exhumation of a Cordilleran-type core complex, although the location and kinematics of the controlling detachment and its relationship with the Busovača Fault are largely unknown. This Miocene fault was inferred to be inverted with a dextral transpressive component during Pliocene times (Hrvatović, 2006).

Previous studies (e.g., Milojević, 1964) have inferred that the continental basin fill was deposited during four main cycles, the timing of their deposition being constrained by an incomplete biostratigraphy (Fig. 2). The deposition of the ~800 m thick Oligocene - Lower Miocene sediments outcropping in the NE part of the basin (Figs. 2 and 3) started with an overall transgression of continental alluvial clastics deposited over an unconformity above the Bosnian Flysch turbidites. The transgression established gradually a lacustrine environment with widespread carbonatic deposition in the basin centre, while thick sequences of coal (i.e. Košćan coal, Fig. 2) alternating with alluvial sediments were deposited in transitional areas. This was followed by a generalized regression and deposition of red alluvial clastics locally overlain by bituminous and porous limestones, as observed in the northern part of the basin. Superposed over this overall pattern, a higher order cyclicity inside these Oligocene - Lower Miocene sediments is suggested by the observed alternation between alluvial clastics, coal deposition and shallow water carbonates. Previous interpretations have inferred the deposition of at least two cycles during this time span, separated by a sub-aerial unconformity (Muftić, 1965; Milojević, 1964).

The deposition of the second, ~1500 m thick, Lower-Middle Miocene sedimentary cycle (Fig. 2) started most probably not earlier than 17 Ma (de Leeuw et al., 2012). The onset of a new transgression is documented by the dominant deposition in a paludal and marshy environment, where nine coal seems were accumulated and are intercalated with continental clayey sandstones and mudstones that are ultimately overlain by shallow water lacustrine limestones. These are further overlain by the gradual onset of a laterally variable sequence that starts with thin bedded marls and silts. These are gradually and laterally replaced by sandstones and conglomerates in a coarsening upwards pattern. This coarse part of the basin fill is named Lašva Series and changes laterally from thick conglomerates of up to 1000 m thick to a few hundred metres thick alternations of sandstones and marls towards the SE (Milojević, 1964). The clastic material was derived from the Bosnian Flysch in the NE and Mid-Bosnian Schist Mountains in the SW (Jovanović et al., 1971). These sediments are overlain by the Koševo Series composed of marls, coals and limestones that indicate a gradual drowning of a swamp environment and the creation of a perennial lake (Milojević, 1964). These deposits are overlain by the 200 m Orlac conglomerates and 200 m Pliocene alluvial sediments. The latter were deposited over a larger area transgressing over the Mid-Bosnian Schist Mountains (Milojević, 1964). The present geometry of the basin shows generally younger sediments towards the SW. The exception is the Upper Miocene - Pliocene deposits that are observed in synforms (or "depressions") in the north, south and western margin of the basin (Fig. 3).

3. Methodology

The excellent exposures together with good lateral continuity of outcrops in the Sarajevo-Zenica Basin have allowed the correlation of fault kinematics with depositional history. The mapping was

Tectonic system tract	Age of depositional cycle	Description	Thickness (m)	Lithostratigraphy	Tectonic events
POST - RIFT	Pliocene	Alluvial series: clay, sand and pebble	200		SW NE
POST - RIFT	Late Miocene	Orlac conglomerate: massive finegrained conglomerate interbedded with sandstone and limestone	200		
POST - RIFT	Late Miocene	Koševo series: marlstone, limestone, clayly sandstone, clay and coal	500-800		
SYN - RIFT	Lower - Middle Miocene	Lašva serie: conglomerate and sandstone interfinger with marlstone and limestone	600-1000		SW NE
SYN - RIFT	Lower - Middle Miocene	Transition zone: thinly bedded marlstone alternating with sandstone and conglomerate	400-800		
PRE - RIFT	Oligomiocene	Main coal series: 7 coal layers intercalated with sandstone, marlstone and clay	350-550		SW NE
PRE - RIFT	Oligomiocene	Porous bituminous limestone	50-200		
PRE - RIFT	Oligomiocene	Red series: conglomerate, sandstone and marlstone	100-500		
PRE - RIFT	Oligomiocene	Košćan coal seam within platy limestone, sandstone and marlstone	100-300		
PRE - RIFT	Oligomiocene	Basal zone: conglomerate, sandstone and limestone	10-100		

Legend:

basement

- Bosnian Flysch

- Mid - Bosnian Schist Mountains

basin fill

- coal seams intercalated with sandsone, marlstone and clay

- alternation of conglomerate, sandstone, marlstone

- conglomerate and sandstone intercalated with/without marlstone, limestone

- coal seams intercalated with platy limestone, sandstone and marlstone

- alternation of marlstone, limestone, clayly sandstone, clay and coal

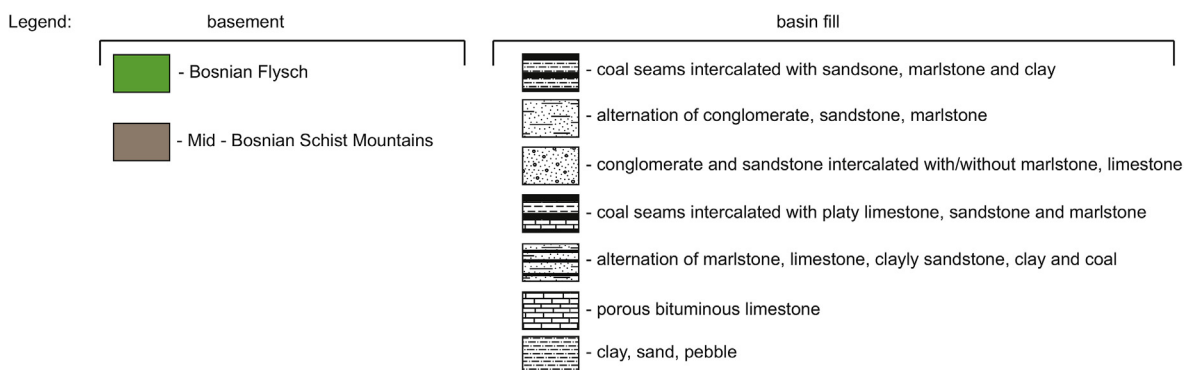- porous bituminous limestone

- clay, sand, pebble

Fig. 2. Tectonostratigraphic column of the Sarajevo − Zenica Basin. Stratigraphic ages, description, depositional cycles, thickness and lithostratigraphy modified after Milojević (1964). Tectonic system tracts and events are results of the present study.

performed along cross-sections by following the main valleys cross-cutting the basin. These were correlated by a large number of isolated outcrop observations (Fig. 3). The sense of shear along faults and shear zones was derived from common kinematic indicators such as Riedel shears, drag folds or slickensides. The relative timing of deformation was defined based on cross-cutting, stratigraphic and offset relationships. The syn-kinematic deposits are commonly observed as clastic wedges in the hanging-wall of normal faults, footwall or hanging-wall of thrusts sealed by fine-grained sediments. Whenever the size of syn-kinematic wedges was larger than the outcrop (i.e. the post-kinematic sedimentation not visible in outcrop), the wedges were detected based on variable offsets across faults, which decrease upwards in the stratigraphy. When deformation structures and their associated syn-kinematic wedges were tilted by subsequent tectonic events, their geometry was restored by using the positions of conjugate normal or reverse faults and/or the attitude of immediately overlying strata. Note that this original attitude could have been close to horizontal in the case, for instance, of a deltaic plain or prodelta, or inclined up to 30° in the case of original sedimentological slopes such as deltaic fronts. We have separated tectonic phases based on the type of deformation and higher-order tectonic events based on consistency of kinematics with stratigraphic time (Fig. 4).

The detailed sedimentological study was based on field mapping and logging of facies units in cross-sections across the basin with special focus on lateral prolongation of facies units, the geometry of syn-kinematic deposits and stratigraphic surfaces. Facies units were defined based on sedimentary structures and textures, geometry, upper/lower boundaries, thickness, fossil content and color (Table 1, e.g., Leppard and Gawthorpe, 2006; Ielpi, 2012). These facies units were subsequently grouped in facies associations (Table 2, e.g., Melchor, 2007; Strachan et al., 2013). Following a typical sequence stratigraphic approach (e.g., Jackson et al., 2005), stratigraphic surfaces were identified based on the contact type between facies associations, associated depositional trends and subsequent stratal terminations across boundaries.

Similar with other sequence stratigraphic studies in tectonically active regions (e.g., Hinsken et al., 2007; Răbăgia et al., 2011), we have used a combination of different sequence stratigraphy techniques to define genetically related strata (i.e. systems tracts) and to correlate them with observed tectonic events. The evolution of the depositional environment during episodes of enhanced tectonic activity was defined using transgressive-regressive sequences (sensu Embry and Johannessen, 1992). The first step was grouping retrogradational-progradational facies associations. Converting these geometrical patterns into transgressive-regressive
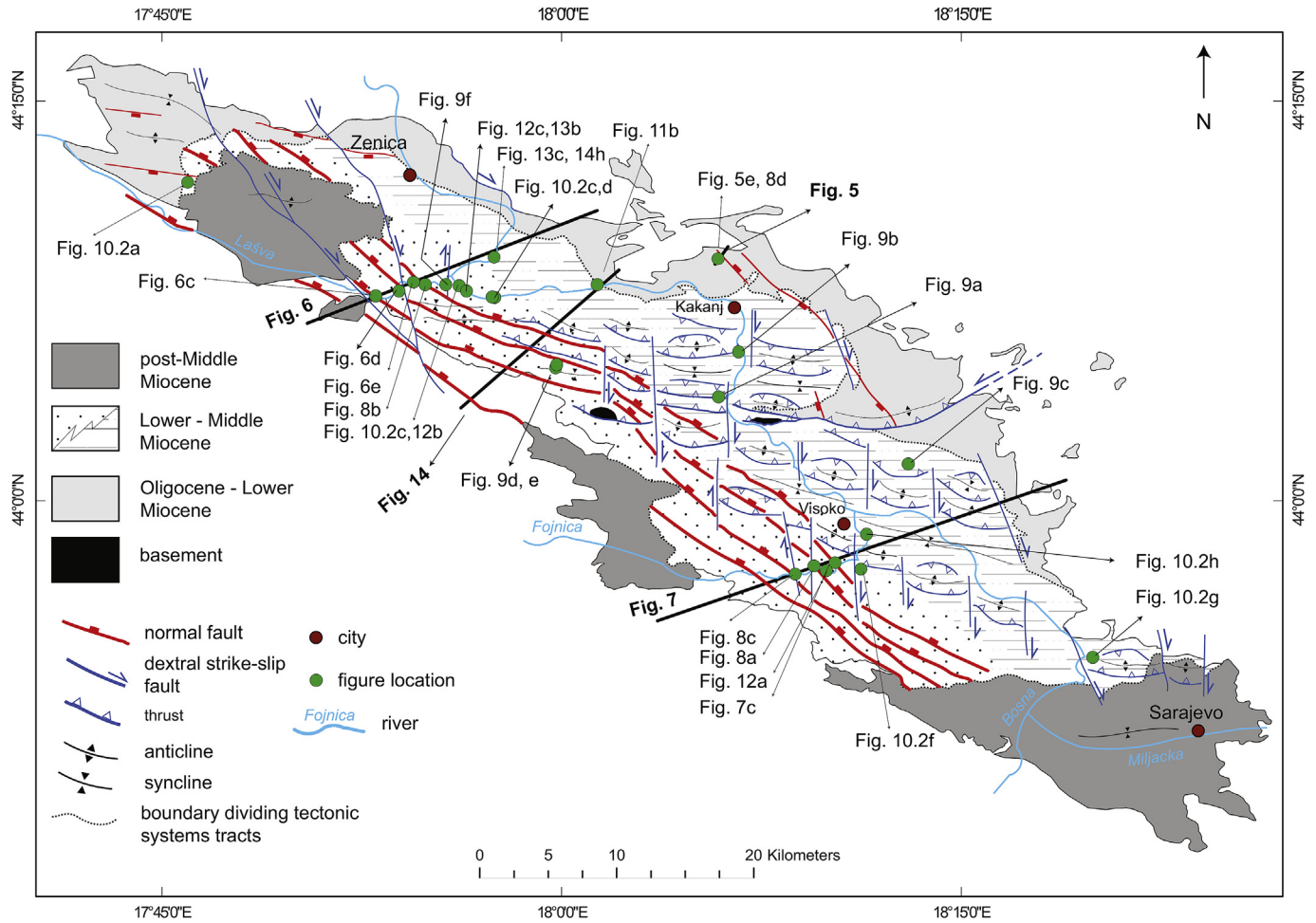
Fig. 3. Simplified kinematic and sedimentological map of the Sarajevo-Zenica Basin (modified from Milojević, 1964 with the results of the present study) with structures active during different deformation events. The Oligocene - Lower Miocene depositional cycle formed in response to the first phase of contraction. The Lower-Middle Miocene depositional cycle formed in response to the phase of extension. The post-Middle Miocene depositional cycle formed in response to the last phase of contraction. Thin black arrows, lines and green dots mark the locations of the profiles and outcrops in Figs. 5–9 and 14. (For interpretation of the references to colour in this figure legend, the reader is referred to the web version of this article.)

stratigraphic sequences relies on the specific structural evolution of asymmetrical extensional systems that creates continuous footwall exhumation and a gradual migration of faulting in time and space. As long as erosion is detected over the footwall, the onlap of the lacustrine facies units is coastal. This corresponds generally with the sub-aerial erosion and coastal deposition observed in studied outcrops. Therefore, a direct interpretation of these geometrical patterns in stratigraphic sequences is possible: the sub-aerial erosion, combined with the coastal onlap and the correlative maximum regression surface, defined by the geometry of the facies associations (e.g. Helland-Hansen and Martinsen, 1996), is an expression of the composite surface that bounds a Transgressive – Regressive (TR) sequence (Embry and Johannessen, 1992). The syn-kinematic deposition against gradually migrating normal faults provides the control over the coeval nature of erosion and sedimentation, whenever available. The maximum flooding surface was defined in the field by downlapping patterns of distal facies associations (e.g., Posamentier and Allen, 1993; Jackson et al., 2005). Such a downlapping surface was observed only in a few places. Whenever this was not available, the maximum flooding surface was approximated as the transition between retrogradational and progradational depositional trends. Such an approximation affects

inherently the definition of individual systems tract, but not the one of sequences.

The correlation between kinematic and sedimentological observations was done extensively for the Middle - Late Miocene extensional phase that still retains a large number of syn-kinematic deposits observed in outcrops. The Oligocene - Early Miocene and Latest Miocene - Pliocene contractional phases retained just a few syn-kinematic geometries and, therefore, are less described in our sequence stratigraphic analysis.

4. Basin kinematics

Three phases of deformation were recognized in the basin. The first NE-SW oriented phase of thrusting (Fig. 5) and basin subsidence was followed by large scale NE-SW and E-W extension (Figs. 6–8). The last N-S shortening phase (Fig. 9) was characterized by variable structures across the basin.

4.1. Initial shortening

The first deformation phase (Fig. 4a) was characterized by NE-SW contraction observed only in Oligocene - Lower Miocene
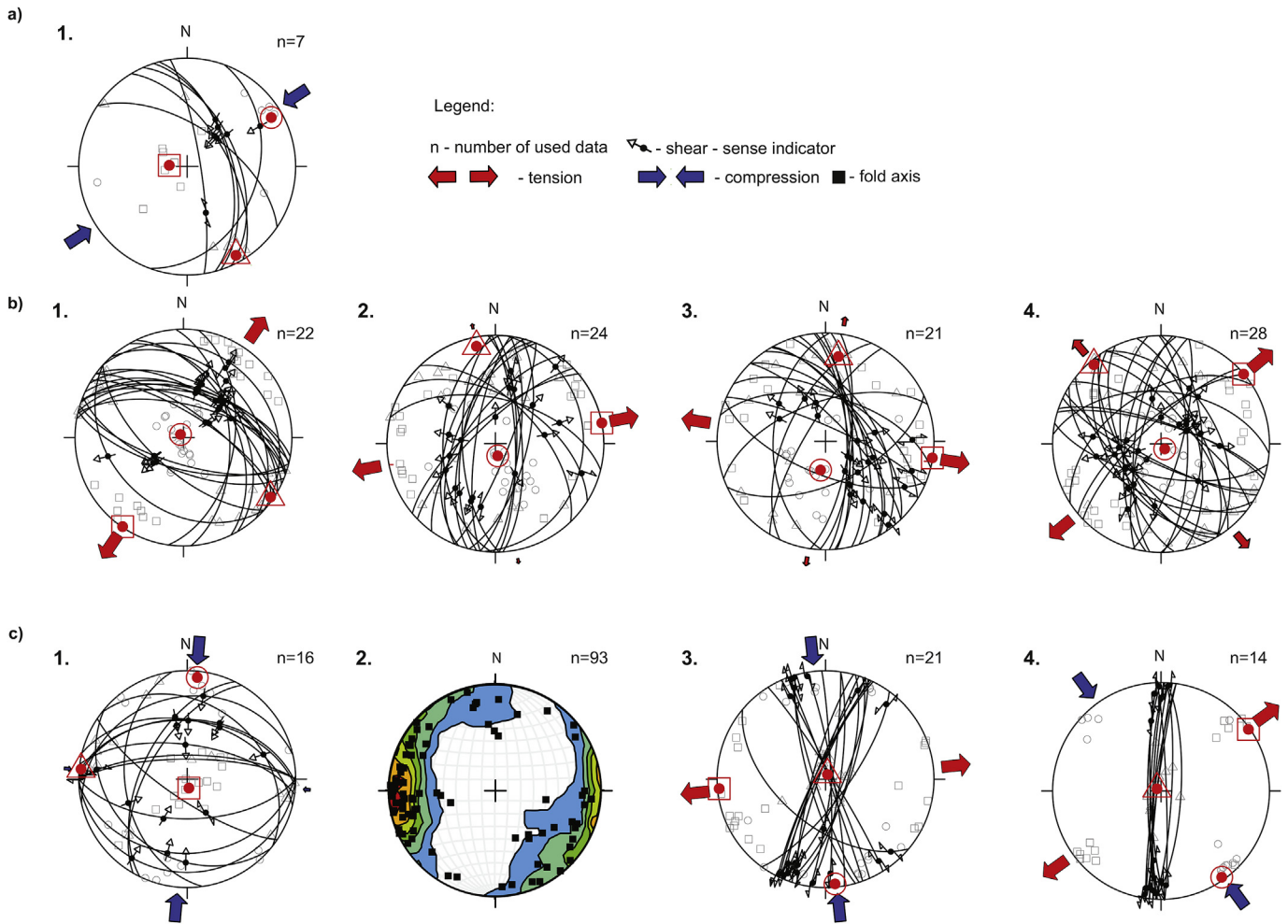
Fig. 4. Kinematics of deformation phases and individual tectonic events recorded in the Sarajevo – Zenica Basin. a) Stereoplot with faults associated with the Oligocene – Lower Miocene phase of contraction; b) Stereoplots with faults formed during the Middle Miocene phase of extension. 1–3 are the individual normal faulting events detected by our study: 4 – normal faults observed in older sediments without separating individual events; c) Stereoplot of structures formed during the Late Miocene – Pliocene phase of contraction, 1 – stereoplots of reverse faults; 2 – stereoplots of fold axes; 3 – stereoplots of strike-slip faults; 4 – stereoplots of transfer/tear strike-slip faults formed due to the inversion along oblique ramps. Red circles, triangles and squares are projections of the mean compressional, intermediate and tensional stress for each fault set calculated using PBT method (e.g., Delvaux and Sperner, 2003). Grey circles, triangles and squares are projections of the measured p, b and t axes, respectively, for each fault in the data set. (For interpretation of the references to colour in this figure legend, the reader is referred to the web version of this article.)

strata that outcrop along the NE basin margin. Locally, clear syn-kinematic depositional wedges and onlaps over the flank of thrusts and anticlines demonstrate that shortening was coeval with sedimentation. Typical structures can be observed in the Bijele Vode profile (NE of Kakanj, Figs. 3 and 5a), where contraction along oblique-slip NNW-SSE trending thrusts with a top SW sense of transport was associated with syn-kinematic deposits onlapping the hanging-wall of faults (Fig. 5a, b). These syn-kinematic wedges thin and pinch-out in the hanging-wall of thrusts. The reverse fault concentrated its slip along the rheological contrast between basin limestones and soft mudstones and is observed as a fine-grained foliated fault gouge with shear-bands characterized by a brittle S-C fabric (Fig. 5c). Other thrusts are associated with the formation of clastic wedges and are sealed by subsequent deposition of finer grained sediments, while onlaps and pinch-outs show syn-kinematic character (Fig. 5e). The overall profile shows intense deformation with tilted strata (Fig. 5b). Similar thrusts or high-angle reverse faults with oblique components of movement were observed also elsewhere along the NE margin of the basin (Fig. 4a), although syn-kinematic indicators of deposition were not always obvious.

4.2. Large scale extension

The second phase of deformation observed (Figs. 3 and 4b) was extensional and resulted in the formation of normal faults that rarely display an oblique component of movement, either sinistral or dextral. Exceptionally well-developed Lower - Middle Miocene syn-kinematic sediments were observed in the Lašva Series, where the normal faults were buried beneath uppermost Miocene - Pliocene deposits and exhumed by subsequent inversion. The syn-depositional character of faults is recognized by the observation of clastic wedges in the hanging-wall, usually covered by fine-grained sediments (Figs. 6 and 8). Faults have variable orientations and gradually changed kinematics with time and along their strike (Fig. 4b), but the dominant strike of large offset faults that control the variations in thicknesses and formation of large sedimentary wedges is NW-SE and N-S with a dominant top-NE to E sense of tectonic transport. Normal faults cross-cutting older pre-kinematic sediments generally show a large spread of extension directions (Fig. 4b4). The stratigraphic correlation of syn-kinematic wedges has allowed the separation of three successive events during this extensional phase (Fig. 4b1-3). These events are in fact the
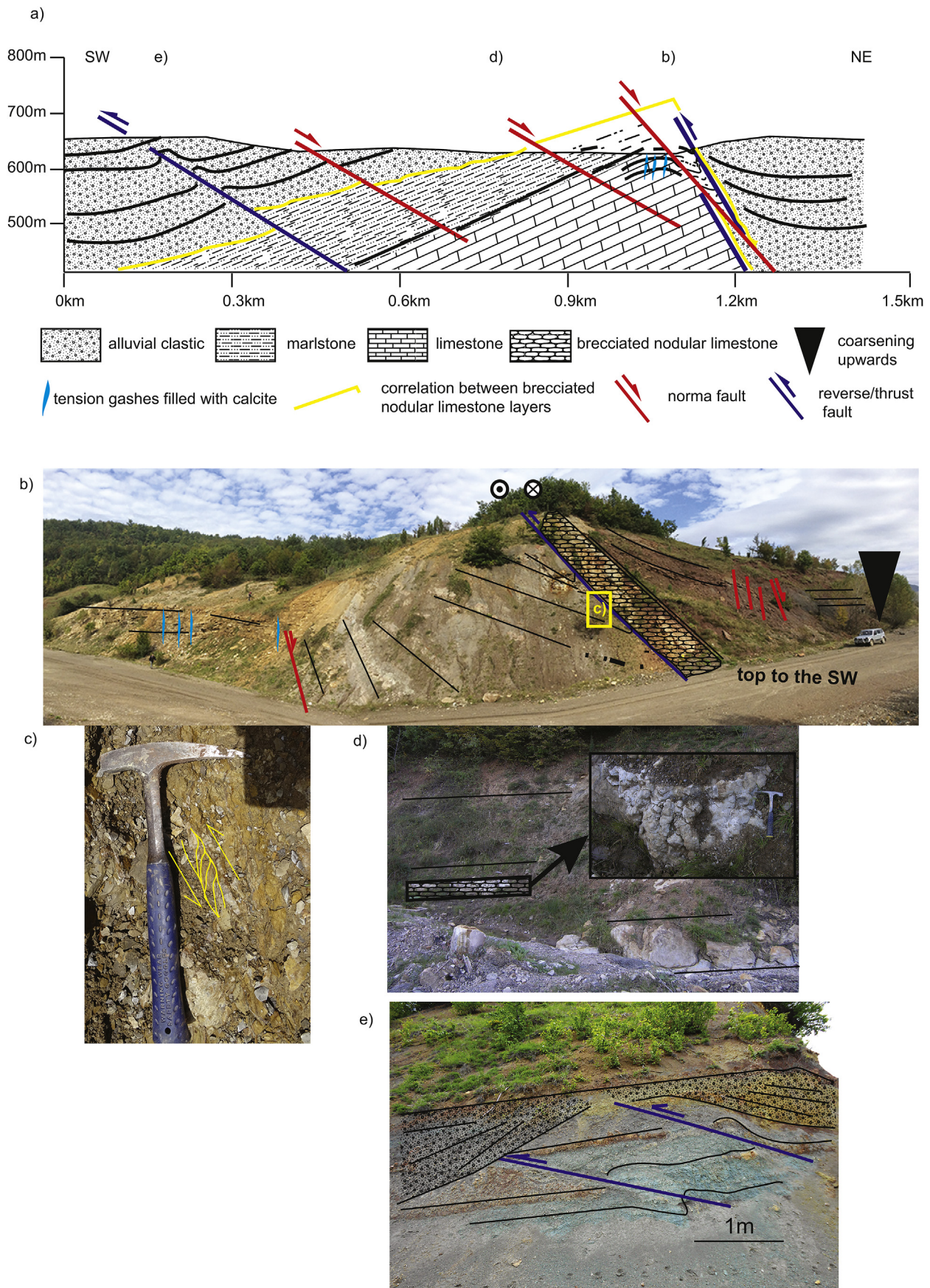
Fig. 5. Example of syn- and post-depositional structures formed during the first phase of thrusting. a) geological cross-section along the Bijele Vode profile, location in Fig. 3. Note the syn-depositional reverse faulting; b) Reverse - sinistral fault (top SW) in Oligocene − Lower Miocene sediments with onlapping of syn-kinematic siliciclastic sediments over the earlier deposited shallow-water limestones. Oblique slip normal faults with lower offsets post-date the deposition. Location in Fig. 5a; c) Detail on the kinematics of the main reverse fault in Fig. 5b with layer parallel slip accommodating the shearing along brittle shear-bands with S-C fabrics developed in poorly consolidated sediments; d) Brecciated nodular limestone intercalated within a mudstone matrix that was deposited at the same time with the limestones in Fig. 5b. The overall structural geometry shows asymmetric folding with SW vergence. e) Syn-depositional reverse faulting within the Oligocene − lower Miocene alluvial sediments. Location in Fig. 5a.
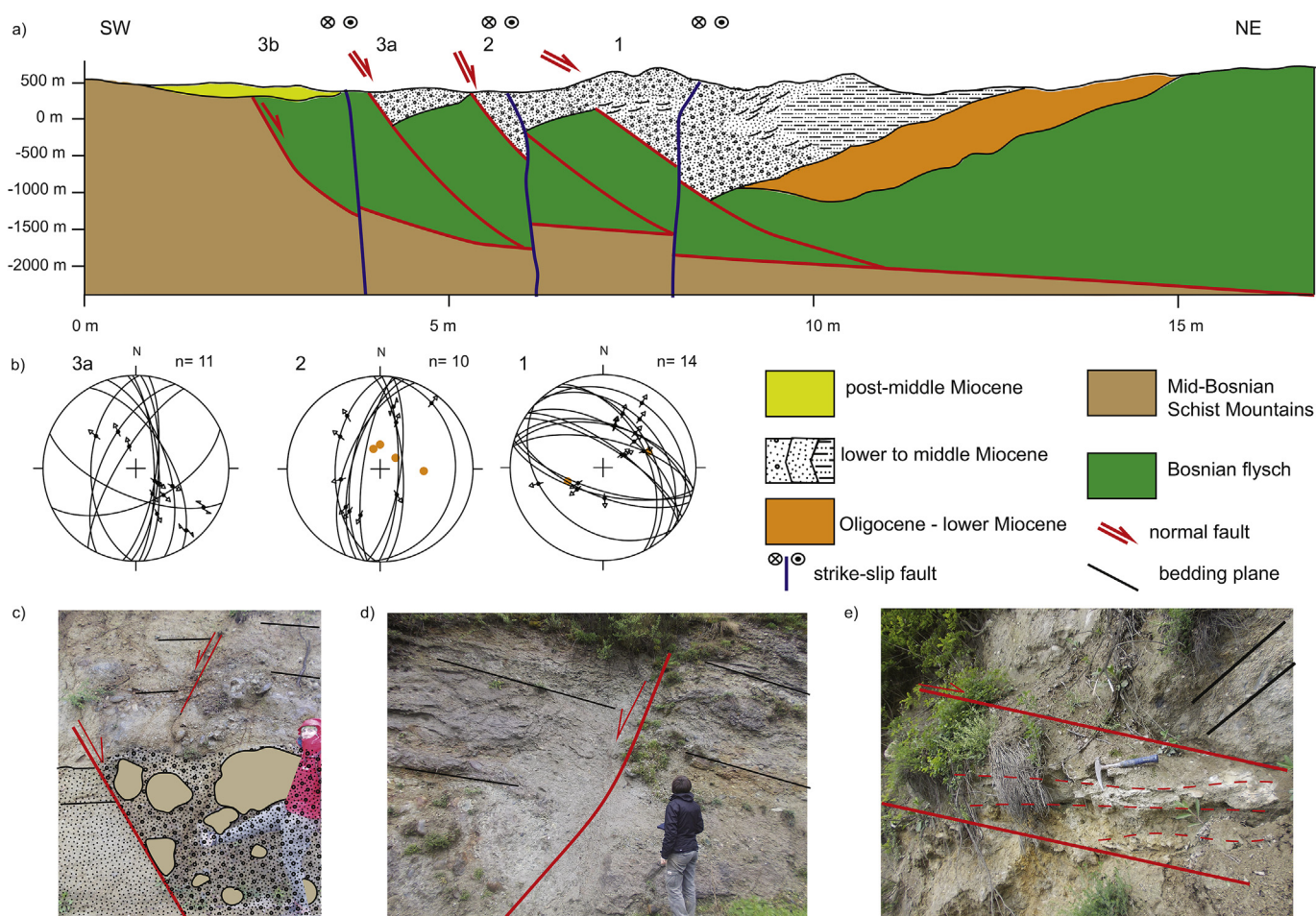
Fig. 6. Example of syn-depositional structures formed during the middle Miocene extensional phase. a) Geological cross section along the Lašva valley with normal faults formed during the three individual events. Note that structure 3b is the Busovača Fault that is not exposed along the profile. This fault was interpreted based on basin geometry and geophysical surveys by previous studies (Hrvatović, 2006). The numbering reflects the evolution in time of normal faulting; b) Stereoplots of normal faults formed during the extensional phase for extensional deformational phase, 1 – first event of normal faulting; 2 – second event of normal faulting; 3 – third event of normal faulting. Orange dots represent pole of the bedding plane used to back-tilt the fault; c) syn-kinematic wedge formed against a normal fault in coarse conglomeratic deposits; d) Listric normal fault with a low degree of subsequent tilting; e) Normal fault with a high degree of subsequent tilting. (For interpretation of the references to colour in this figure legend, the reader is referred to the web version of this article.)

progressive evolution of a normal fault set (consisting of three main faults) branching from a common, nearly horizontal detachment located at the base of the Bosnian Flysch (see below). Such a high-resolution mapping of kinematics and fault evolution with time was possible because the separation of these events and grouping of faults is based on the superposition of the numerous available syn-kinematic wedges with stratigraphic time and not on the consistency of extensional directions.

The first event of normal faulting (Fig. 4b1) indicate a NE-SW extensional direction with limited deviations likely related to local rotations around vertical axis during the subsequent phase of latest Miocene - Pliocene contraction. These faults have large off-sets, usually more than 10 m, but locally exceed the 10–20 m scale of outcrop observation. These faults were also tilted by subsequent normal faulting near the SW margin of the basin or by later contractional thrusts and folds. The second event of extension was generally ENE-WSW oriented (Fig. 4b2). The normal faults have NW-SE to NNE-SSW strikes with a significant component of oblique slip along N-S oriented faults (Fig. 4b2). In outcrops, the inclination of these faults range from 25° to 70°, but this value becomes always around 60° after back-tilting of bedding to its original depositional position. This indicates that similar oriented extensional faults

were subsequently tilted by the last extensional event or the subsequent phase of contraction. The third event of normal faulting indicates ESE- WNW oriented extension (Fig. 4b3), fault orientation showing deviations from N-S to NNW-SSE with oblique slip to strike-slip components of movement. These faults indicate less to no subsequent tilting from their original 60° dip in rheologically strong lithologies, such as conglomerates, near the SW margin of the basin.

Normal faults have planar or listric surfaces defining high or low-angle fault planes with respect to the (tilted) stratigraphy (Fig. 8). High-angle normal faults dip 50–60° in conglomerates. Whenever fault gouge material is made up by softer sediments (such as marls), it forms a clear foliation subsequently truncated by a shear fabric showing a kinematic direction of transport (Figs. 6e and 8a). A large number of normal faults display low angle segments in the soft sediments, particularly well visible in the NE part of the basin (e.g., Fig. 8b). This indicates either original low-angle normal faulting in rheologically weak sediments (LANF segments, e.g., Pedrera et al., 2012) or subsequent exhumation of the listric low-angle level of normal faults. The latter is visible by faults becoming listric and low-angle at rheological contrasts. This geometry is observed, for instance, as decollements accommodating
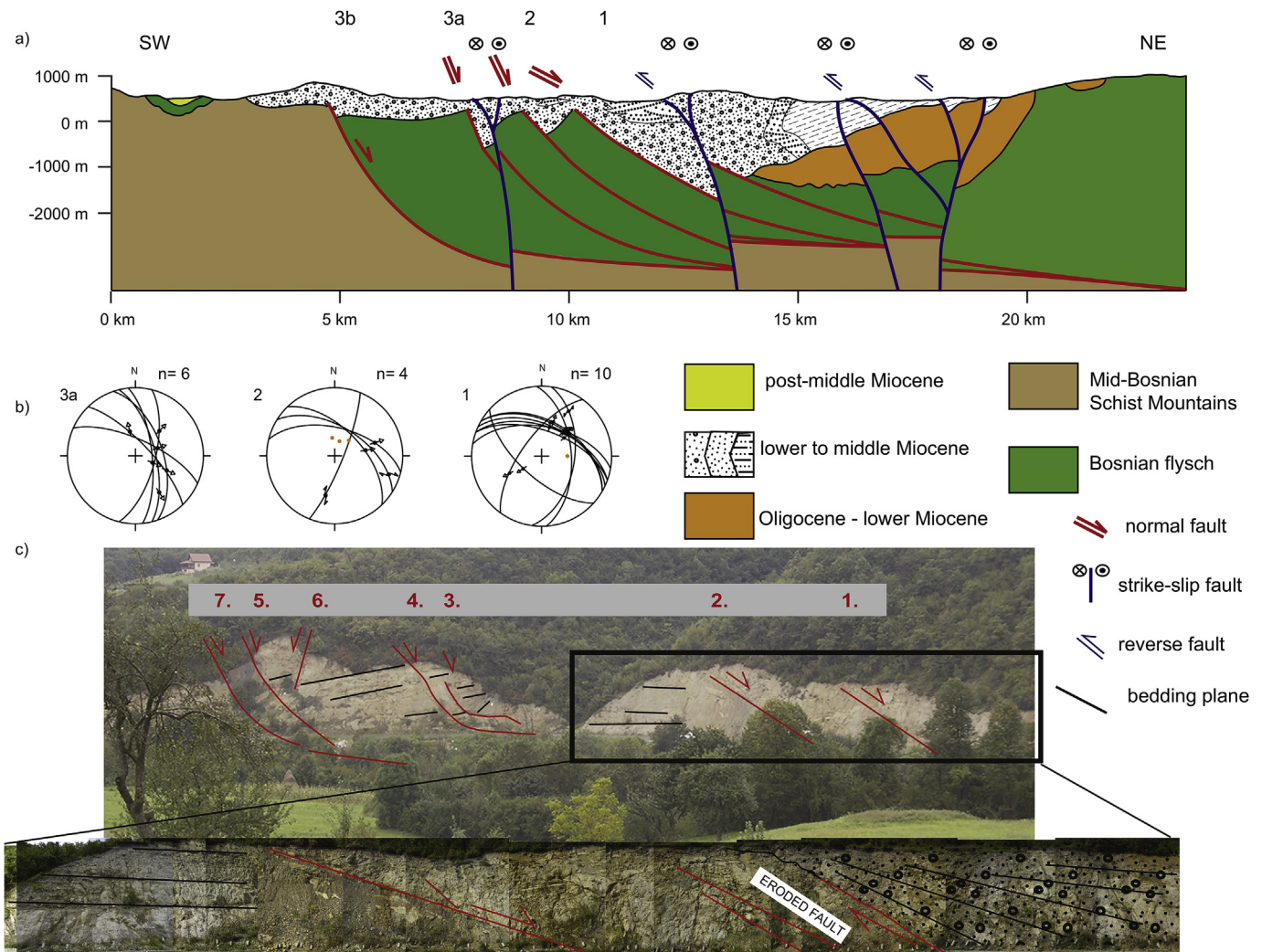
Fig. 7. Example of syn-depositional structures formed during the middle Miocene extensional phase. Location of the profile and outcrops are marked in Fig. 3. a) Geological cross section along the Fojnica valley with the normal faults formed during the three extensional events. Note that structure 3b is the Busovača Fault that is not exposed along the profile. This fault was interpreted based on the basin geometry and geophysical surveys by previous studies (Hrvatović, 2006). The numbering reflects the gradual evolution in time of normal faulting; b) Stereoplots of normal faults formed during extensional events, 1 − first event of normal faulting; 2 − second event of normal faulting; 3 − third event of normal faulting. Orange dots represent pole of the bedding plane used to back-tilt the fault; c) Interpreted photo illustrating a syn-kinematic clastic wedge formed above an eroded normal fault footwall. (For interpretation of the references to colour in this figure legend, the reader is referred to the web version of this article.)

penetrative layer-parallel shear at the contact between coarse (and thick) sedimentary units, such as conglomerates and sandstones, and fine (and thin) sedimentary units, such as siltstones and mudstones (Fig. 8b). Low- and high-angle normal faults intersect and provide crosscutting criteria in syn-kinematic wedges (Fig. 8b). Normal faults locally truncate earlier syn-kinematic wedges associated with the Oligocene - Early Miocene thrusting and their associated unconformities (Fig. 8d). In such situations, tilting of sediments during thrusting can be differentiated from the one created by the subsequent normal faulting. The listric normal faults dipping NE-wards show a gradual migration of deformation towards their SW-ward located footwall, demonstrated by the superposition of syn-kinematic wedges (Figs. 7c and 8c). This is a critical observation that is valid for the extensional phase at the scale of the entire basin. It can be best studied in two profiles constructed along the main valleys crossing the basin, i.e. the Lašva and Fojnica (Figs. 6 and 7). In these profiles, the superposition of syn-kinematic wedges demonstrates that faulting gradually migrated in a footwall direction towards the youngest Busovača Fault. Outside this fault, the geometrical relationships show that

numerous outcrop-scale normal faults are generally connected to three major structures at depth that cumulate larger offsets, which correspond to the three successive deformation events (1−3 in Figs. 6a, b and 7a, b). The average normal fault strike is NW-SE with top NE-transport direction indicating an average NE-SW extension, although many variations are observed including oblique and strike-slip faults (Figs. 6b and 7b). The syn-kinematic sedimentation is frequently coarse conglomeratic and is associated with smaller-offsets synthetic and antithetic normal faults (Figs. 6c and 7c). Faulting was associated with significant footwall uplift, which is documented by erosion of fault planes that removed large parts of the overlying coarse conglomeratic deposits (Fig. 7c). This erosion created gentle slopes buried by subsequent prograding wedges. The overall offsets are variable from few centimetres to more than 10 m (e.g., Fig. 8). Hanging-wall antithetic rotations tilted previously formed faults and their footwalls, which resulted in lower inclinations of synthetic fault planes against inclined bedding (Fig. 7a). The cumulative offset of all normal faults observed is in the order of 1 km, which corresponds roughly with the stratigraphic thickness of the Lašva unit in the proximal conglomerate area.
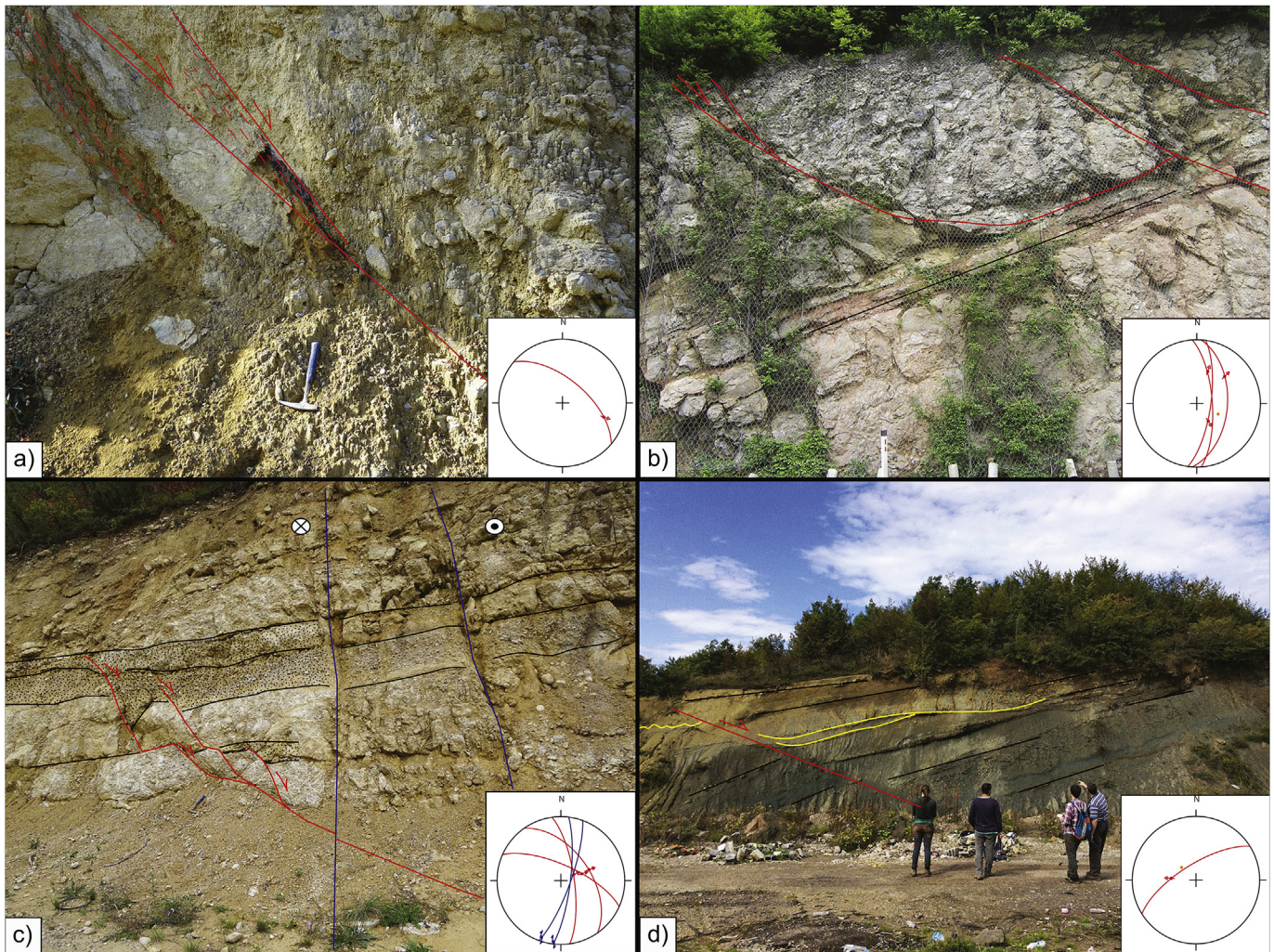
Fig. 8. Field examples of the relationship between normal faulting and sedimentation. Location of outcrops is shown in Fig. 3. Note the orange dots represent pole of the bedding plane used to back-tilt the fault. a) Fault gouge with internal cataclastic foliation in unconsolidated clays and sandstones within syn-kinematic conglomeratic deposits; b) Listric ramp-flat geometry truncated by subsequent higher angle normal faults in syn-kinematic conglomeratic deposition. The decollement layer is made up by siltstones; c) Back-stepping migration of normal faulting at outcrop scale in syn-kinematic deposition. The latter are visible by a wedge geometry in the local deposition; d) A top to the NE normal fault cross-cutting the pre-kinematic Oligocene continental clastics with paleosoil horizons marking the bedding (black line) and lacustrine marls deposited above an erosional unconformity (yellow line). (For interpretation of the references to colour in this figure legend, the reader is referred to the web version of this article.)

When adding the offset of the SW-most fault that could not be estimated (Figs. 6a and 7a), the total offset is likely much higher.

4.3. Final basin inversion

The third deformational phase (Fig. 4c) produced reverse faults, asymmetric folds and a large number of tear faults that affected both the underlying basement and its Mesozoic cover, and the overlying basin fill (Fig. 3). The overall contraction direction is N-S oriented, observed both in faults and folds, with a large number of deviations along structures that display local strain partitioning. This is caused by inversion along oblique ramps, which in fact are the dominantly NW-SE striking normal faults formed in the previous deformation phase. In the basin, this oblique thrusting created a large number of tear faults as observed by N-S striking dextral faults (Figs. 3 and 4c3-4) formed by thrusting over the NW oriented segments of oblique ramps. They are also associated with sinistral conjugate faults with comparatively smaller offsets.

The N - S to NNW-SSE contraction was also accommodated by a large number of folds that are observed mainly in the finer turbiditic or deep-water pelagic sequence, while the coarse grained sequence deformed mainly by thrusting. Individual folds are symmetric, tens of meters wide with generally E-W oriented axial planes (Fig. 4c2), often with hinge collapse or parasitic folds along their flanks (Fig. 9a). When associated with thrusts, folds become asymmetric (e.g., Fig. 9c), with axial planes of variable inclinations from 20 to 80°. Thrusts vergence is both N- and S-wards. Shortening accommodated by folding is variable, as indicated by wide and open anticlines and synclines that laterally change into tight and overturned folds formed near major thrusts characterized by ramp-flat geometries (Fig. 9c). Decollement levels, i.e. flats, are usually localized in finer sediments (shales, silts) that are deformed in wide shear zones with shear-bands like geometry (Fig. 9b) accommodating large (i.e. tens of meters) layer parallel offsets. Folding was associated with the local formation of a pervasive cleavage that was subsequently sheared in the footwall of major thrusts (Fig. 9d).
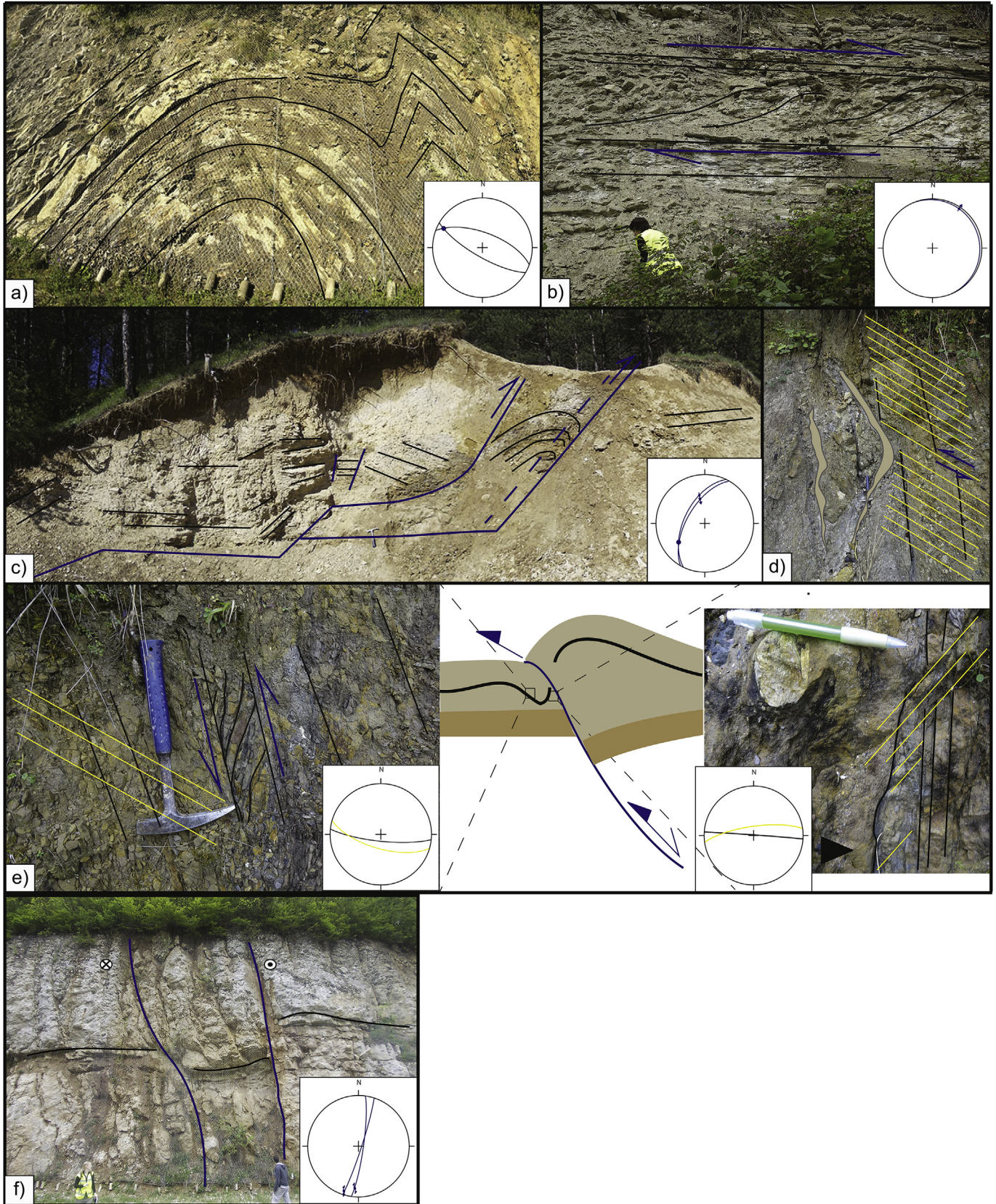
Fig. 9. Interpreted photos with field examples illustrating the last Late Miocene − Pliocene phase of basin inversion. Location of outcrops is shown in Fig. 3. The black lines represent bedding planes, yellow lines are cleavage and blue lines depict fault planes. a) typical folding patterns in central basin turbidites with the core of the anticline associated with hinge collapse and parasitic folding; b) layer parallel shear in silts and marls with drag-folding along the flat part in a typical ramp-flat thrusting geometry; c) ramp flat geometry of a thrust deforming middle Miocene deposits; d) Reverse shear along a cleavage plane associated with minor folding; e) layer parallel shear zone (left) associated with the formation of cleavage (right) in the footwall syncline of an inverted normal fault. Some of the pre-existing normal faults in the basins retained normal slip at depth associated with anticlinal growth in the younger successions. The black triangle represents the fining upward trend; f) Outcrop example of a negative flower structure with dextral NW-SE oriented slip. At regional scale, it represents a tear fault accommodating slip along a lateral ramp truncating earlier deposited conglomerates. (For interpretation of the references to colour in this figure legend, the reader is referred to the web version of this article.)

5. The evolution of sedimentary environments during the Early − Middle Miocene

The Early-Middle Miocene sedimentary infill consists of successions of alluvial-deltaic conglomerates and sandstones (Lašva series of Milojević, 1964) that are laterally replaced with more distal prodelta lacustrine turbidites, slumps, or more profundal lacustrine deposition (the Transition zone of Milojević, 1964). The sedimentological mapping has separated 18 facies units (Table 1), which are grouped in the 13 facies associations (Fig. 10, Table 2) described below.

5.1. Alluvial fan system

The alluvial system is well observed along the entire SW margin of the basin, usually juxtaposed against eroded fault scarps. The overall geometry shows wedging, thickening towards the footwall and pinching out in the opposite hanging-wall direction. The size of wedges is highly variable, from tens of meters to tens of decimetres. The more proximal part of the alluvial system can be generally described by two facies associations (A1 and A2, Table 2).

The proximal alluvial fan facies association A1 consists of pebble to boulder breccias and conglomerates (Figs. 10 and 11a). The base of this facies is a sharp boundary and/or erosional unconformity and is gradational towards the adjacent facies associations (A2 and B1). The angularity and clast size suggest a short distance transport.

This is in agreement with clast composition, which corresponds to the metamorphic and magmatic lithologies of the neighbouring Mid-Bosnian Schist Mountains and their Mesozoic cover. Giving the usual location in the immediate hanging-wall of normal faults, this facies association formed due to fault scarp degradation and deposition by rockfalls and debrisfalls (e.g., Postma and Drinia, 1993; Leppard and Gawthorpe, 2006).

The proximal to middle alluvial fan facies association A2 is composed of amalgamated sheets of pebble to cobble size conglomerates and coarse-grained sandstones (Fig. 10). Laterally, these conglomerates are interbedded with or overlain by thin layers of fine sandstones and siltstones that contain often water escape structures. The latter structures together with the large grain size and high angularity of clasts indicate rapid deposition near the source area from unconfined sheet floods and mass flows events in the proximal to middle alluvial fan environment (e.g., Nemec and Steel, 1984; Miall, 1985). Laterally, the A2 facies association is inter-bedded with or overlain by B1 and B2 associations.

Facies association B1 comprises of conglomerates and sandstones which are usually amalgamated, cutting each other vertically and laterally forming multi-storeys bodies (Table 2, Figs. 10 and 11b), where each store is bounded by an erosional surface and preservation of the fine-grained intercalations is low. Laterally, B1 passes into B2 facies association. The B2 facies association includes laminated siltstones and claystones intercalated with thin layers of organic rich clay or isolated channels of fine- to medium-grained sandstone and

Table 1
Lithofacies units separated in the Sarajevo-Zenica basin. The codes used and their interpretation follow the general standardisation described in previous sedimentological studies (Bouma et al., 1962; Postma, 1990; Miall, 1996; Talling et al., 2012).

facies units	description	interpretation
Gcm	clast-supported cobble (boulder) to pebble size (breccia) conglomerates with low amount of granula matrix; subangular to subrounded clasts; poor sorting; massive; plane base	cohesionless debris flow, granular flow
Gmm	matrix-supported cobble (boulder) to pebble size (breccia) conglomerates in fine sand/mud matrix; subangular to subrounded with/without chaotically distributed mud clasts; poor sorting; lack of vertical grading; non-erosional base with sharp grain size break at the boundaries; bed thickness varies from 0,4 to 1,5 m, very often amalgamated beds with thickness >10 m	cohesive debris flow
Gh	clast- to matrix-supported pebble to cobble size conglomerates; moderate sorting; weak normal grading, sometimes no grading; crude horizontal stratification; planar base; bed thickness varies from 25 to 40 cm with lateral extension tens of meters	sheet flood deposits, longitudinal bars, lag deposits
Gp	clast- to matrix-supported cobble to pebble conglomerates; subrounded to rounded; weak sorting; planar-cross bedding, imbrication; erosional bases; bed thickness varies 0,3 −1,3 m	transverse bedforms
Gt	clast- to matrix-supported pebble to cobble conglomerates; subangular to subrounded; through cross-bedding; weak sorting; erosional basal surface; graded or ungraded; bed thickness varies from 0,3 to 2 m	channel fill
Sr	coarse to fine sandstones; well sorted with ripple cross-lamination; thickness of bed set is <20 cm	ripples-lower flow regime, overbank stream-flood deposits
Sm	medium to coarse grained sandstones; poorly sorted; no internal structure with/without scattered granulas and pebbles	subareal to subaqueous cohesionless debris flow;
Sh	fine to coarse grained sandstones; horizontal bedding; slightly erosional base; beds 7−20 cm thick	plane-bed deposits under subaerial sheet flows or stream flows
St	medium- to fine-grained sandstones; well sorted; rounded clasts; weak normally graded or ungraded; solitary or grouped cross-bedding	megaripple under subareal sheet flows or stream flows
Fl	fine sandstones interbedded with siltstones and mudstones sometimes with scattered granulas; laminated or massive; bed set thickness less than 10 cm	deposition from suspension of waning floods or abundant channel
Ta	coarse- to medium-grained (pebbly) sandstones with low matrix content; medium to good sorting; vertical normal grading or no grading; mud chips aligned in certain levels; erosive or planar base	high density turbidity currents
Tb	medium-grained sandstones; parallel lamination; poor vertical overall grading	high/low density turbidity currents
Tc	medium- to fine-grained sandstones; well sorted, low matrix content; asymmetric ripple cross-lamination/climbing ripples; laminae can be convoluted; tapering shape of sandstone beds; sometimes the steeper sides of ripples are draped by organic matter	low density turbidity currents
Td	fine sandstones to siltstones; parallel lamination result of the alternation of 1−2 mm thick fine sandstones and siltstones laminae; can resemble FU grading trends	low density turbidity currents
Te	fine siltstones and mudstones; not stratified, but may exhibit parallel lamination marked by well sorted silt; dark grey to light grey color	suspension fall-out from waning low density turbidity currents or cohesive density flow
L	beige mudstones; laminated with wavy to planar bedding; upper and lower boundaries are sharp and plane; sometimes can be mottled with reddish fakes; lens body geometry; include fossil fragments (ostracods); thickness varies from >1 to 15 cm	lagoon, shallow lake to back-swamp suspension, background deposition
Md	mudstones, light brown; lack of internal structure; no fossils; tabular with gradual contact with units above and below; bed thicknesses is up to 1 m	inorganic lake precipitation

Table 2
Summary of facies associations interpreted in the Sarajevo-Zenica basin.

Depositional environment		Facies associations code	Facies code (see Table 1)	Description	Inferred depositional process
Alluvial fan	proximal	A1	Gcm, Gmm	Wedge-like packages of red structureless coarse-grained conglomerates with variable amounts of matrix. Angular to subangular basement-derived clasts varies from 2 cm to 2 m in size with scarce blocks of 2,5 to 3 m. Tectonic (i.e. fault scarps) or erosional contact towards the adjacent basement or basin fill. It may exceed 20 m in thickness. Locally truncates A2 and B1.	Colluvial rockfall and debrisfall deposits originated from variable degree of rolling and sliding of fragments down the slope before deposition. They are deposited in the lower part of the slope (fault escarpment). The lithological nature of the clasts suggests small catchment area restricted to BSMts (footwall, e.g., Postma and Drinia, 1993; Longhitano et al., 2015).
		A2	Gmm, Gcm, Sm, Sh, minor Gp, Sr, Gh	Sheet-like packages of red coarse-to medium-conglomerates intercalated with coarse-grained sandstones. Subrounded to subangular polimictic clasts may show imbrication. The lower and upper boundaries are plane and slightly erosional. Thickness varies from 2 to 5 m. Locally truncates B1 and B2.	Deposition from flood-related braided flows dominated by sheet flows combined with debris flows. This association of depositional processes is typical for deposition in the proximal to middle alluvial fan (e.g., Miall, 1985; Nemec and Postma, 1993).
	distal	B1	Gp, Gcm, Sm minor Gh, Sh	Channelized to sheet like packages of red medium-to fine-grained conglomerates and sandstones with scarce siltstones. The lower and upper boundaries of channelized conglomerates and sandstones are wavy and erosional. The sheet-like packages show subhorizontal bedding marked by abrupt change in the grains size.	Deposition from dominantly subareal braided-stream flows and sheet flows, rarely intercalated with debris flow deposits i.e. high-energy and bedload dominated flows in the bride-plain environment (e.g., Nemec and Postma, 1993).
		B2	Sm, Fl, Sh, St	Tabular packages of (wavy or parallel) laminated siltstones and (organic-rich) claystones intercalated with finegrained sandstones. The siltstones and claystones may have mudcracks or iron crust and/or be mottled. They are irregularly intercalated with poorly sorted medium-grained sandstones and granula-conglomerates. The geometry of these intercalations varies from channel- to lobe- and sheet-like. Alternates with B1 and C0.	Deposition from subareal waning flows combined with suspension fall-out in the overbank environment often interrupted by flooding events (e.g., DeCelles et al., 1991; Ielpi, 2012).
Pond/shallow water lake system		C0	Fl, L, Sh, Sm	Lense-like packages of (wavy or parallel) laminated beige mudstones intercalated with single bed, or subordinately bed sets of fine- to medium - grained sandstones or angular granula conglomerate. The mudstones can be bioturbated with mottled upper surface. The mudstones include Ostracodes.	Deposition by particle settling in low energy environment; lagoon or ponds in the marginal lake environment with rare debris flows resulting from flood events (e.g., Melchor, 2007; Ielpi, 2012)
Deltaic system	delta plain	C1	St, Gcm, Sh, Sr, Gt	Channelized packages of trough-cross bedded medium- to coarse-grained conglomerates interbedded with sheetlike packages of coarse- to medium-grained sandstones and conglomerates. The clasts are subrounded to rounded. The channel lag comprises of pebble to cobble size conglomerates. The layers thickness varies from 0.5 to 2 m. These layers are intercalated with thin (up to 20 cm) medium- to fine-grained sandstones with wavy and ripplecross lamination. The packages are organized in the coarsening- and thickening-upward sequences. Gradually passes into D1 downslope.	The thick layers of sandstones and conglomerates were deposited from stream, sheet and debris flows recording periods of bedload river floods at the river mouth. The sandy intercalations resulted from lower flow regime, waning flows or by reworking during periods of quiescence (e.g., Colella, 1988; García-García et al., 2006).
	delta slope	D1	Gcm, Sm, minor Ta-c	Sheet-like packages of coarse- to medium-grained conglomerates and sandstones. The bed thickness varies from 0,3 m to 2, 5 m. The scattered pebbles (even boulders of BSMts) suggest horizontal bedding in amalgamated beds. They are interbedded with 5–15 cm thick fine-grained sandstones and siltstones.	Combination of multiple depositional processes: dominated by the debris flow, grain flow and lesser influence of turbidity currents typical for aggradational and progradational delta slope. The flows originated by hyperpicnal mixing of river and lake water due to high sediment input during fluvial flooding events (e.g., Prior and Bornhold, 1988; Colella, 1988).
		D2	Gcm, Sm, Ta-e	Channelized to sheet like packages coarse-to medium- grained sandstones engulfed in fine-grained sandstone to siltstones. Package thickness varies from 3 m to 5 m. The package show coarsening- and thickening-upwards.	Deposition dominantly from high energy and concentrated turbidity and debris flows on the erosional slope of a delta (e.g. Leppard and Gawthorpe, 2006).
	proximal prodelta	E1a	Sm, Gmm, Ta-e	Sheet- to wide lobate and channel - like packages of coarse- to medium-grained sandstones, siltstones and mudstones with rare influxes of medium-to fine-grained conglomerates with/without rip-ups. Subordinately, this unit may include lobe-like geometry of the layers and slumped intervals. This is a downslope equivalent of D1.	Deposition from turbidity currents and debris flow deposits in the toe of the slope, proximal prodelta settings (e.g., Leppard and Gawthorpe, 2006; Strachan et al., 2013).

		Description	Interpretation
E1b	Sm, Ta-e	Isolated channel-like layers of medium-grained sandstones interbedded fine-grained sandstones, siltstones and mudstones. The succession may be interrupted by poorly sorted coarse-to medium-grained sandstones with the intrabasinal rip-up or out-sized clasts. It may contan plant remains and coal particles. The package coarsens and thickens up-section. Upslope it passes into D2.	Deposition from unidirectional subaqueous turbiditic currents interrupted with debris flows. The channel-like geometry and intrabasinal rip-ups suggest erosional slope (e.g. Leppard and Gawthorpe, 2006).
E1c	Ta-e	Sheet-like packages of parallel to wavy laminated fine- to medium-grained sandstones and siltstones intercalated with mudstones. This packages include slumped layers with variable thicknesses from 0.25 cm to 15 m. The slumped layers contained intrabasinal rip-ups, blocks and folded beds. Laterally truncates D2 and E2b.	Deposition from alternating of high - and low-density turbidity flows intercalated with mass flows resulted from slope instability (e.g., Postma, 1984; Strachan et al., 2013).
distal prodelta E2a	Ta-c, L, Md	Parallel to wavy laminated beige mudstones regularly interbedded with well-sorted medium-grained calcarenite sandstones. The sandstones are structureless with plane base, sometimes may show coarsening-upwards and/or, parallel lamination and/or ripple-cross lamination. The sandstones comprises of dominantly Ugar flysch fragments (limestone) with subordinate amount of organic matter and coal particles. The mudstones contain ostracodes. The whole succession is irregularly interrupted with structureless mudstones up to 1 m thick. Usually, this facies association forms a base of coarsening upwards sequence gradually passing into E1b.	Combined deposition from low-density turbidity currents and suspension fall-out with cyclic high-density turbiditic flows in the distal prodelta environment. The lithic fragments in cyclic sandstones suggest catchment area restricted to pre-rift coal-rich succession and Ugar flysch (e.g., Benvenuti et al., 2007; Melchor, 2007).
E2b	Tc-e, Md	Sheet-like packages of parallel laminated mudstones intercalated with fine-sandstones, siltstones and ripple crosslaminated sandstones associated with organic-rich mud drapes. Bed thickness varied from 5 to 15 cm. This facies association includes Ostracodes.	Cyclic alternation of low density-turbidity currents and suspension fall-out in the distal prodelta and basin plane setting of the underfilled basin (with low sedimentary input, e.g. Melchor, 2007)

pebbly sandstone crevasses (Table 2). The immersion surfaces are marked by red iron-rich crusts and mottled structures developed in silts and palustrine carbonates. The channelized system of B1 facies association has an unconfined character and was deposited in a high energy/discharge braided plain of a delta fan (e.g., Nemec and Postma, 1993). Furthermore, B2 facies association are floodplain deposits deposited in a quiet, low energy environment, with confined channels in the braided plain delta fan (e.g., Miall, 1985; Pavelić and Kovačić, 1999). The distal fan facies often alternates with the C0 facies association described below, which may be the result of avulsion of distributary channels, increasing the sediment discharge due to flooding, or cyclic activity of normal faults (e.g., Gawthorpe and Colella, 1990; DeCelles et al., 1991).

5.2. Pond/shallow water lake system

The facies association C0 is composed dominantly of thinly bedded mudstones interrupted by isolated channel-like coarse sandstones and breccias (Table 2, Figs. 10 and 11c). Sometimes, it may contain mottled top part of a layer. This facies association often has a wedge geometry, rarely includes lenses, and is thickening towards the centre of the basin. It is usually intercalated between B2 and C1, and is frequently downlapped by the B1 facies association. Red alteration layers in carbonates indicate local pedogenesis (i.e. mottled, e.g. Ielpi, 2012). The carbonate deposition is often associated with lacustrine ostracods that indicate suspension settling in a shallow lake/pond environment. This is periodically supressed by channels feeding a mouth bar system or occasional flooding events (e.g. Melchor, 2007).

5.3. Deltaic system

Facies association C1 consists of channelized and tabular conglomerates and sandstones (Table 2, Figs. 10 and 11d) usually organized in coarsening and thickening upward packages. The observed erosion, trough cross-bedding and finning upwards indicate migration of channels and bars under hyperpycnal flow in the place where a river discharges in a body of stagnating water (Fig. 11d) (i.e., a delta plain, e.g. Postma, 1990; García-García et al., 2006).

The facies association D1 consists of cobble to pebble conglomerates and coarse- to medium-grained sandstones (Fig. 10), often marked by outsized clasts of Mid-Bosnian Schist Mountains (Fig. 11e). The flows were induced on the sedimentological slope by discharging a coarse-grained alluvial bedload during flooding events or more likely by grain flow from an unstable delta slope (e.g., Prior and Bornhold, 1988). They show tabular and wide lobate bed geometries parallel to the basin margin and basin tapering wedges along the flow profile. The D1 may have sharp and flat, or gradational contacts to the adjacent facies associations (B1, C1 upslope and E1a down-slope) and general coarsening-upwards trends. D2 facies associations include wide channel to sheet-like coarse- to medium-grained sandstones facies (Fig. 10). Erosion, stacked channels and scarcity of tabular beds indicate deposition from unidirectional flows bypassing and depositing material downstream (e.g., Mulder and Alexander, 2001; Leppard and Gawthorpe, 2006). This can be observed also in the lateral transition to facies association E1a and E1b described below.

Facies association E1a contains dominantly coarse- to medium-grained sandstones interbedded with siltstones and mudstones facies (Table 2, Fig. 10). The tabular to wide lobate and channelized turbiditic layers are interrupted by slumps (Fig. 11f). Slumped layers contain a mixture of coarse grained clasts up to boulder size and rip-up clasts of parallel laminated layers of slope sediments supported by a fine sandstone/siltstone matrix. They represent
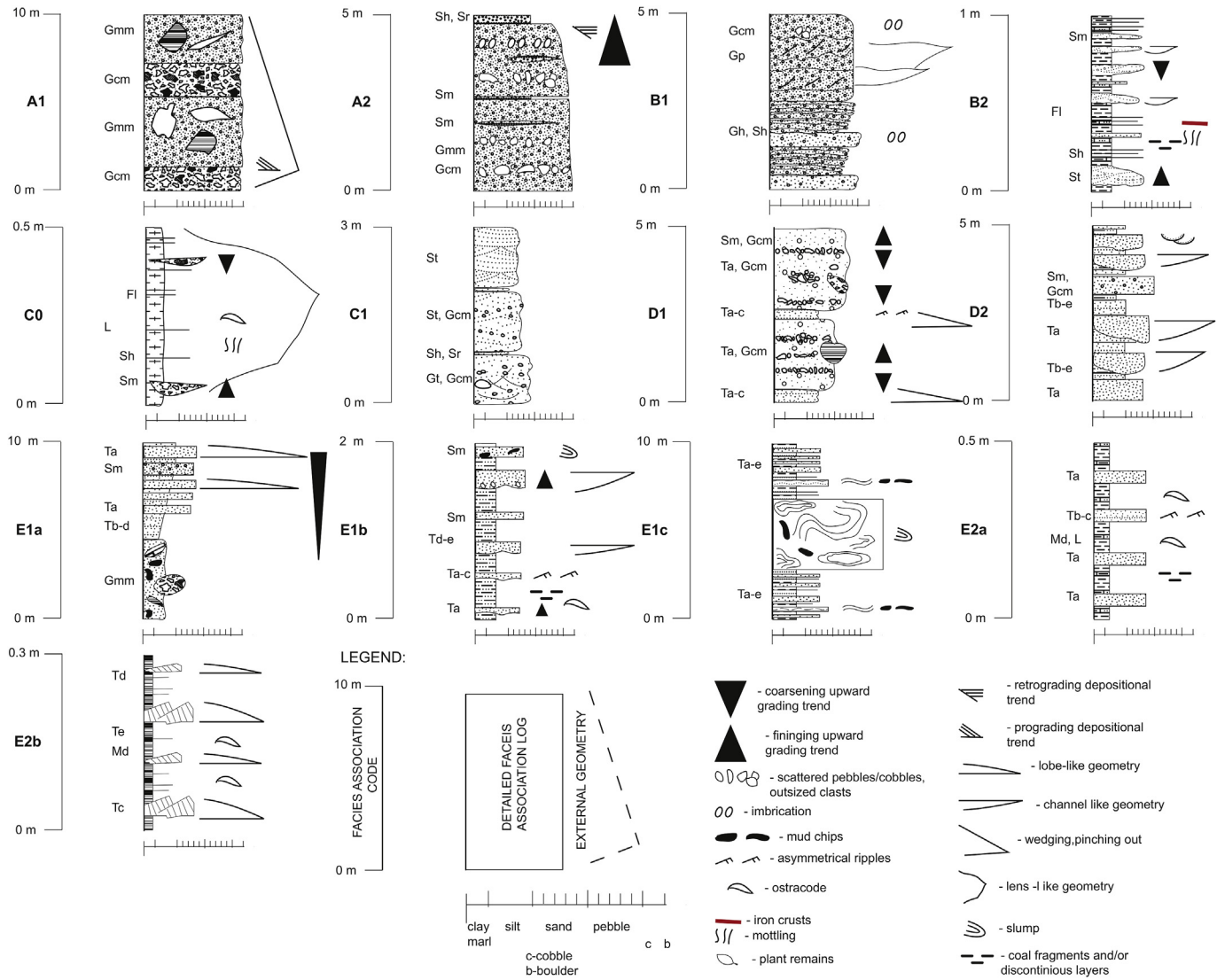
Fig. 10. Grouping of lithofacies units into facies associations.

material that was deposited at the toe of the slope due to avalanching along the unstable steep slope (e.g., Postma, 1984; Strachan et al., 2013). Downwards the slope, E1a gradually passes into E1b.

The E1b facies association is characterized by isolated channel-like sandstones facies engulfed within siltstones and mudstones (Table 2, Figs. 10 and 11g). The sandstones are poorly to medium sorted with subangular to subrounded fragments of schists and limestones. The grain size, thickness and frequency of sandstones increases upwards from fine- to coarse-grained. This means an increase of terrigenous material input by erosion of a rejuvenated footwall and deposition by a feeding system with unidirectional concentrated flows further basin-ward (e.g. Lowe, 1982; Mulder and Alexander, 2001). This is documented by a gradual transition into the E2a facies association downwards along the flow direction. Additionally, plant remains and coal fragments suggest hanging-wall directed input as well, most likely by erosion of the previously deposited Oligocene - Lower Miocene coal series. This facies association has a gradual transition to E1a upwards in the stratigraphy.

The facies association E1c is made up by an alternation of sheet-like medium- to fine-grained sandstones, siltstones and mudstones

facies (Table 2, Figs. 10 and 11i). This monotonous succession is sometimes interrupted by large scale slumps consisting of folded and broken autochthonous/intra-basinal layers or chaotic deposits. This indicates that the unconfined flows in the distal prodelta environment are obstructed by deposits of seismically triggered failure due to local fault activity (e.g., Postma, 1984; Sharp et al., 2000). The facies association E1c grades upslope into D2 and downslope into E2b.

The facies association E2a is made up by alternations of rhythmic sheet-like calcarenite sandstones and mudstones (Table 2, Fig. 10). The majority of the beds are structure-less, indicating deposition from steady turbidity currents with rapid aggradation, in most cases suppressing tractional transport or post-depositional reworking (e.g., Talling et al., 2012; Strachan et al., 2013). This suggests significant reworking of the clastic material in a shallow water environment before deposition into a distal delta environment. Some of these flows may represent the dominance of paleoflows draining hanging-wall composed of Bosnian Flysch limestones. This facies association represents periodic broad terminal channel lobes from a more proximal setting prograding into a mud-prone succession of the distal prodelta (e.g., Benvenuti et al., 2007; Talling et al., 2012).
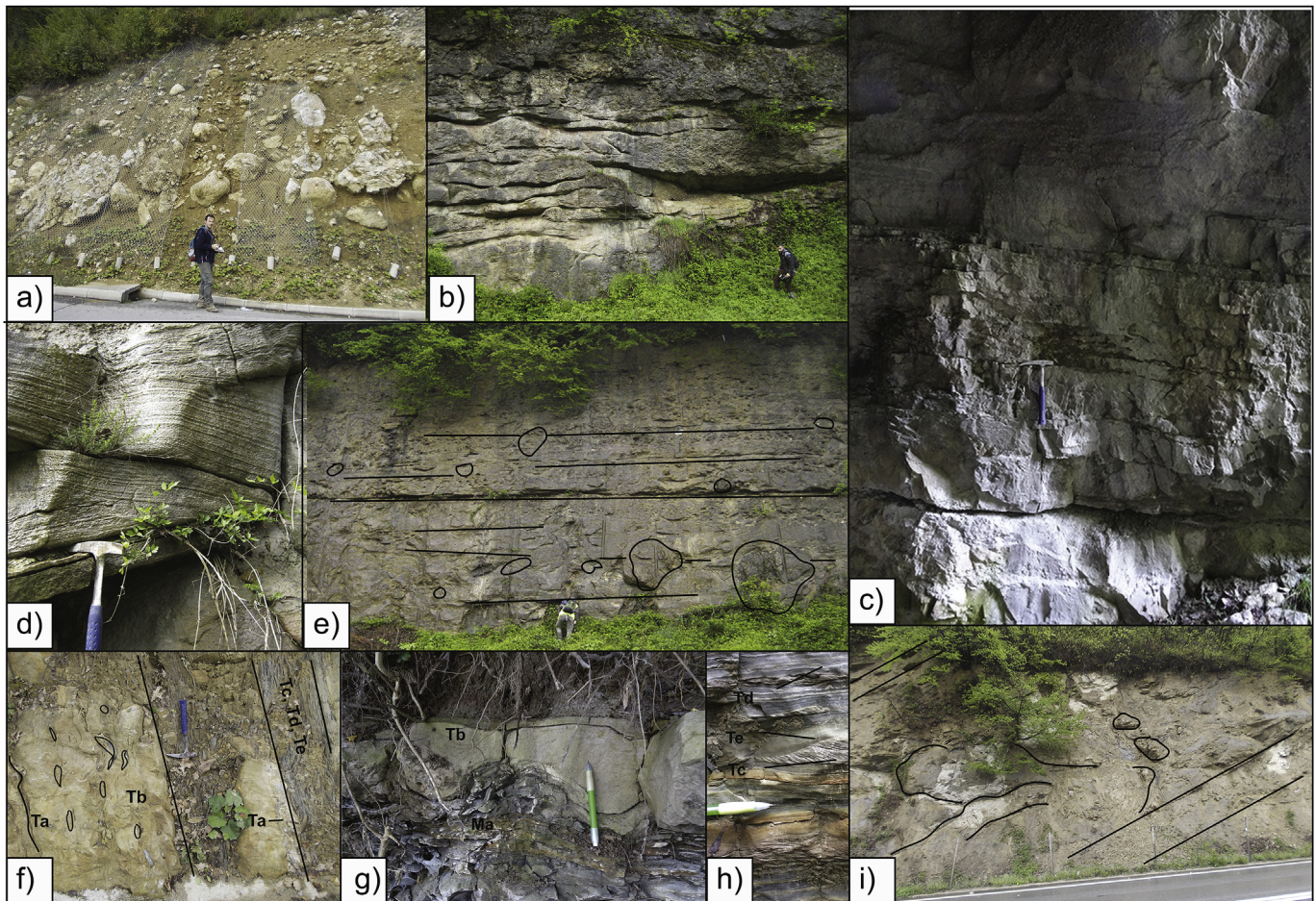
Fig. 11. Field examples of facies associations. Location of outcrops is shown on Fig. 3 a) Example of the debris flow deposits in the proximal alluvial fan facies association A1. Note basement blocks up to 2 m in diameter; b) Sheetflood deposits in the distal part of the fan, facies association B1; c) Example of shallow water carbonates, facies association C0; d) Example of inter-distributary channel and bars facies association C1 with cross-bedded sandstones; e) Example of delta front facies association D1 with outsized clasts (up to 1.5 m in diameter) in a turbiditic sequence; f) Example of toe-slope facies association E1a with sandstone megabeds containing rip-up clasts; g) Example of prodelta facies association E1b with loading structures of fine-grained sandstones over mudstones; h) Example of distal prodelta facies association E2b with starved ripples in distal turbidites; i) Example of prodelta facies association E1c showing slope failure probably caused by fault activity.

The facies association E2b is made up of mudstones sometimes intercalated with medium-grained ripple-cross laminated sand-stones (Table 2, Figs. 10 and 11h). The mudstones contain dark and light grey to orange laminae that formed as a result of variable content of organic matter. The alternation of monotonous dark brown to dark grey mudstone are suggestive to anoxic bottom waters (e.g., Melchor, 2007; Ielpi, 2012). The transition between various mudstones is sharp inferring dominant deposition by settling from suspension at the lake bottom with variable redox conditions. Alternatively, these can also represent low density flows and/or mud debrites in the distal part of a basin floor fan (e.g. Talling et al., 2012). In general, this facies association indicates a lack of terrigenous influx and a dominance of the mud flows in the starved, under-filled basin (e.g. Carroll and Bohacs, 1999). In the stratigraphic succession E2b facies association alternates with E1a or D1 facies associations, and their contacts are sharp.

6. The link between normal faulting and evolution of facies associations

Our observations in the Sarajevo-Zenica Basin indicate a close link between the activation of normal faults and deposition of various facies associations. This link is best described by three characteristic groups of facies associations. These correspond to the evolution of the depositional environment, controlled by the balance between the rate of creating accommodation space and the rate of sediment supply, during the three main stages of a normal faulting: onset (Fig. 12), high displacement rates (Fig. 13) and gradual termination of fault activity (Fig. 14).

The onset of normal fault activity triggers the coeval deposition of A1, A2 and E2b facies associations (Fig. 12). The bulk of deposition consists of proximal to middle fan facies associations localized right next to the normal fault scarp (Fig. 12a, d). The footwall is uplifted during faulting and subsequently providing eroded material for deposition of A1 and A2 facies associations. These facies associations show a prograding and aggrading character in the hanging-wall direction forming a steep talus that may reach 30° inclinations (Fig. 7c). The overlying strata indicate that the alluvial fan incises and erodes the fault scarp, creating a sub-areal unconformity, which is recognized latter as a sequence boundary (Fig. 7c). The coeval deposition in the more distal lacustrine environment is marked by sediment starvation, observed by deep lacustrine deposits conformably overlying pre-faulting littoral limestones (e.g. E2b over pre-faulting strata, Fig. 12b, d). The latter infers rapid basin subsidence (Prosser, 1993). The base of this sequence in deep lake deposits (i.e. E2b) was used as a diagnostic marker for a sequence
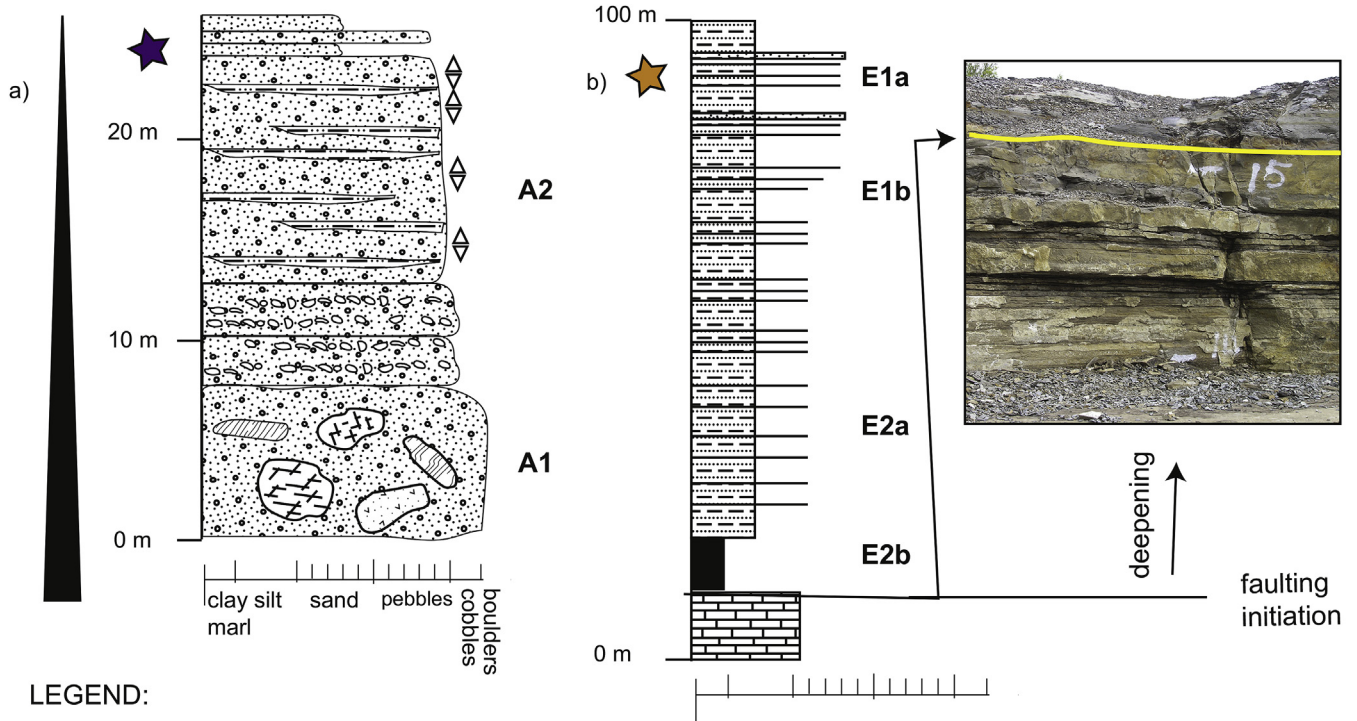
LEGEND:

- limestones (pre-faulting strata)

- conglomerates intercalated with sandstones and siltstones

- alternation of mudstones, siltstones, sandstones

- conglomerates

- organic rich mudstones

NOT TO SCALE
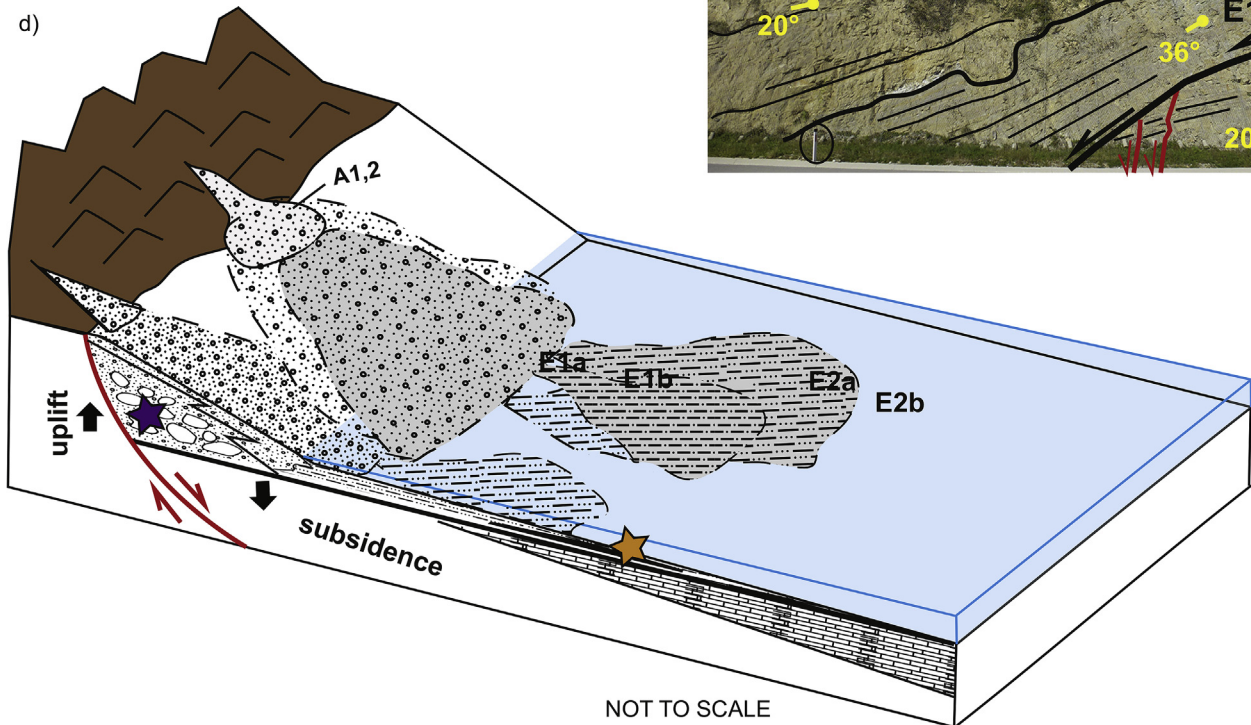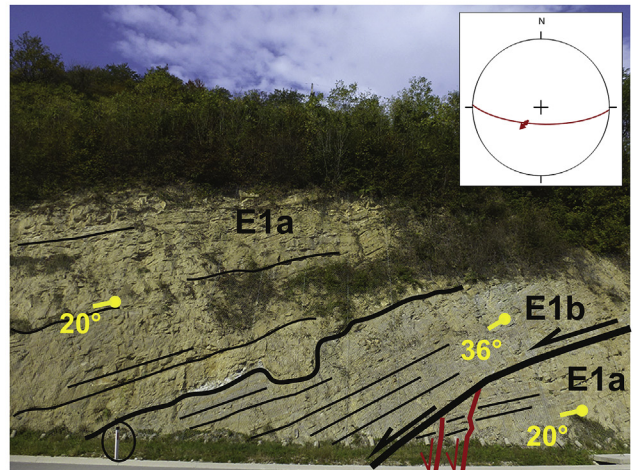
boundary, being correlative to the proximal erosional unconformity marking the maximum flooding surface. Furthermore, the normal fault activation (synthetic and antithetic) is recognized in deep water facies by the presence of large scale slumps (E1c, Fig. 11i), or mud-prone slope deposits (E1b) often overlying an angular unconformity (Fig. 12c). The wedge shape geometry of sedimentary bodies infers higher subsidence rates in the immediate hanging wall, but also may suggests that tilting was controlled by the listric geometry of the normal fault (García-García et al., 2006).

The period of highest displacement rates (Fig. 13) increases the accommodation space rapidly. This leads to simultaneous deposition of immature terrestrial material in the proximal to middle alluvial fan facies associations (A1 and A2) and delta slope (D1, D2 and E1a) settings restricted to a narrow zone in the immediate hanging wall. The progradation of irregular flows of immature terrestrial material in the lake indicates erosion of the steep uplifting footwall and material transport via bypass flows without significant reworking and residence time (e.g. Leppard and Gawthorpe, 2006). Consequently, more distal and lateral facies associations (B1,B2, D2, E1b) record a decrease in channel amalgamation and channel/overbank ratio up in the section, with higher frequency coarsening-upwards influxes within the overall fining-upwards grading trend (Fig. 13a). Such higher frequency influxes may indicate short term flooding-events (e.g. Støren et al., 2010), or short periods of tectonic quiescence and further transport of material eroded from the footwall (e.g. Catuneanu, 2002). Similarly, periodic lobes in the distal prodelta environment (E2a, E2b) can also be interpreted to be transported by flows draining both the hanging-wall and the footwall, or are events of hanging-wall tilting during normal fault activity (Figs. 12b and 13d). The shallow water lacustrine carbonates with Ostracode fauna mark the maximum flooding surface (Fig. 10c, C0 in Fig. 13b, c). The facies beneath this surface show retrogradational and fining upward grading trends (Fig. 13a, c), while the overlying facies associations display progradational stacking patterns and coarsening upwards (Figs. 13b, c and 14b).

The final stage of fault activity (Fig. 14) is characterized by lower rates of creating accommodation space when compared with sedimentation rates and ultimately end of fault activity (e.g. Sweet et al., 2003, 2005). The subsidence of the hanging-wall extent over the immediate footwall at low rates. The effect is that only in the most proximal areas the facies associations A1 is replaced by A2 and B1 in the vertical succession, which onlap the slope and the eroded fault scarp with general retrogradational and aggradational deposition, and fining-upwards grading trends as the fault activity dies out (Figs. 7c and 14a). This retreat is caused by the erosion of the fault scarp and general lowering of the source area relief when the activity of the fault and thereby exhumation of the footwall terminates. In the more distal areas, the accommodation space is outpaced by the sedimentation rate, the effects being observed in the dominance of coarse-grained material, coarsening-upwards grading due to progradational depositional trends accompanied

by low rates of aggradation in the delta plain (Fig. 14b, c, d). Often the vertical succession finishes with smaller fining-upwards trend, especially visible in the distal facies associations. The distal faces associations (C1, D2, E1b) indicate an increase in channel amalgamation and channel/floodplain sediments ratio up in the section (Fig. 14b). Laterally, progradation can be followed along a gradual or sharp transition from E1a,b to D1 facies associations (Fig. 14c). The sediment was supplied by the high energy bedload-dominated rivers that show a gradually decreasing in energy in response to exhaustion of the source area which resulted in small fining-upward packages capping the sequence.

The next faulting event occurs into footwall of the previous fault. The onset of this next event causes drowning of previous deltaic system. The change from prograding to retrograding (syn-kinematic) depositional trend during fault migration is marked by a change at the maximum regressive surface. This migration and subsequent progradation during the next cycle is visible in the basin in an outcrop (Fig. 14e, f).

7. A coupled tectonic and sedimentological model of the Sarajevo - Zenica Basin during the asymmetric Early - Middle Miocene extension

Field observations demonstrate that the second depositional cycle in the Sarajevo - Zenica Basin was dominantly controlled by the Early - Middle Miocene extension. This is proved by the observed features of syn-depositional normal faulting and associated clastic wedges. The response of facies associations (Fig. 15) to each event of normal faulting is rapid overall deepening. The asymmetry of extension created the dominant deposition of coarse proximal delta facies associations against the SW margin of the basin and the deposition of coarsening- and fining-upwards cycles in the vertical profile. In most of the observed situations, rapid changes in facies associations are driven by coeval normal faulting and, therefore, there is a direct link between extensional tectonics and sedimentation. Obviously, this does not completely exclude the influence of other external forcing factors, such as climatic lake level variations driven by the balance between precipitation and evapo-transpiration, which may incorporate questionable global or regional eustatic effects in such an enclosed intra-montane basin (e.g., Leever et al., 2011).

At the level of one extensional event, we interpret the onset of fault activity and the period of maximum displacement rates to correspond to a transgressive systems tract, while the final stage of fault activity corresponds to a regressive systems tract (Fig. 16). They are separated by a maximum flooding surface and together form a TR cycle. These cycles are bounded by a composite surface that includes a sub-aerial unconformity and the correlative maximum regressive surface. In the distal lake facies, the maximum regressive surface may be missing or overlap with the maximum flooding surface due to overlapping activity of the two subsequent faults, such as for instance at the highest displacement rate of one

Fig. 12. Sedimentological evolution of various facies associations of the tectonic systems tract at the onset of fault activity. a) Typical sedimentological log for the proximal units of the onset fault activity systems tracts deposited over eroded fault planes in their hanging-wall; b) Typical sedimentological log illustrating the progradation in deep lacustrine environment at the base of the slope created by the normal faults. This progradation follows the initial transgression recorded over the organic rich marls and is observed as a transition from immature to well-developed turbidites. Note the high amount of organic matter in the mudstones probably reflecting stratigraphic condensation due to rapid deepening. The yellow line marks correlative maximum flooding surface at the base of the new sequence dividing pre-faulting mudstones (E2b) and shallow water carbonates (pre-rift deposits); c) toe slope décollement triggered by antithetic faulting in the basin. The thick black line (i.e. angular unconformity) represents the previous décollement surface. The activity of the normal fault created steep fault scarp and tilting of the pre-existing slope which combined with the basin ward dip of the bedding in the uplifted footwall behaves as a décollement surface. The created accommodation space was partly filled by the prograding and aggrading hanging-wall directed mudflows (E1b). The erosional surface and scouring (wavy black line) at the top of the E2b suggests erosional and bypass flows before higher amount of coarse material (E1a) fill up the previously created space and decrease the slope gradient. The scale of the outcrop is shown by the traffic sign (0.7 m high) in the black. The red line with arrow on the stereoplot indicates orientation of the fault plane and sense of movement; d) Interpreted sedimentological environment combining the A, E1 and E2 facies associations. See Fig. 10, Tables 1 and 2 for the meaning of the facies association codes. (For interpretation of the references to colour in this figure legend, the reader is referred to the web version of this article.)
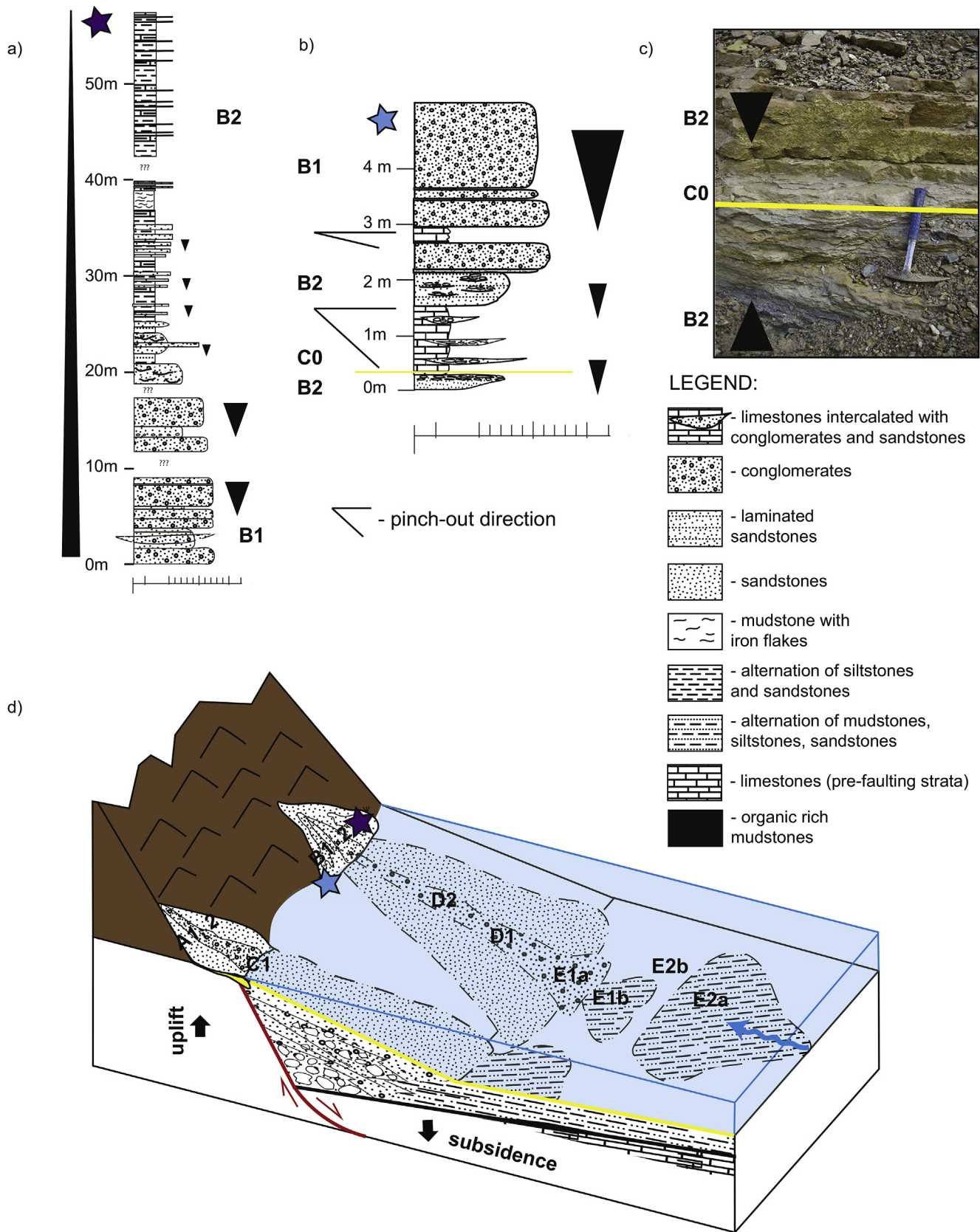
Fig. 13. Sedimentological evolution of various facies associations of the systems tract formed during highest displacement rates of faults. a) typical sedimentological log of distal fan facies deposited during the rapid transgression associated with the subsidence of the normal faults hanging-wall. An upward transition from channelized distal alluvial fans to flood plains and shallow lacustrine deposition is observed; b) Sedimentological log illustrating a maximum flooding surface formed during the highest displacement rates of normal faulting, observed by shallow water lacustrine carbonates rich in ostracodes separating a distal alluvial facies associations. See also Fig. 12c; c) isolated crevasses and channels in overbank deposits (lower part of the section below yellow line). The amount of the channels and crevasses increases up in the section. These are separated by a maximum flooding surface marked by shallow water limestones with ostracodes (yellow color); d) Interpreted sedimentological environment combining the A, B, C and E facies associations. The blue arrow suggests hanging-wall directed drainage. See Fig. 10, Tables 1 and 2 to for the meaning of the facies association codes. (For interpretation of the references to colour in this figure legend, the reader is referred to the web version of this article.)
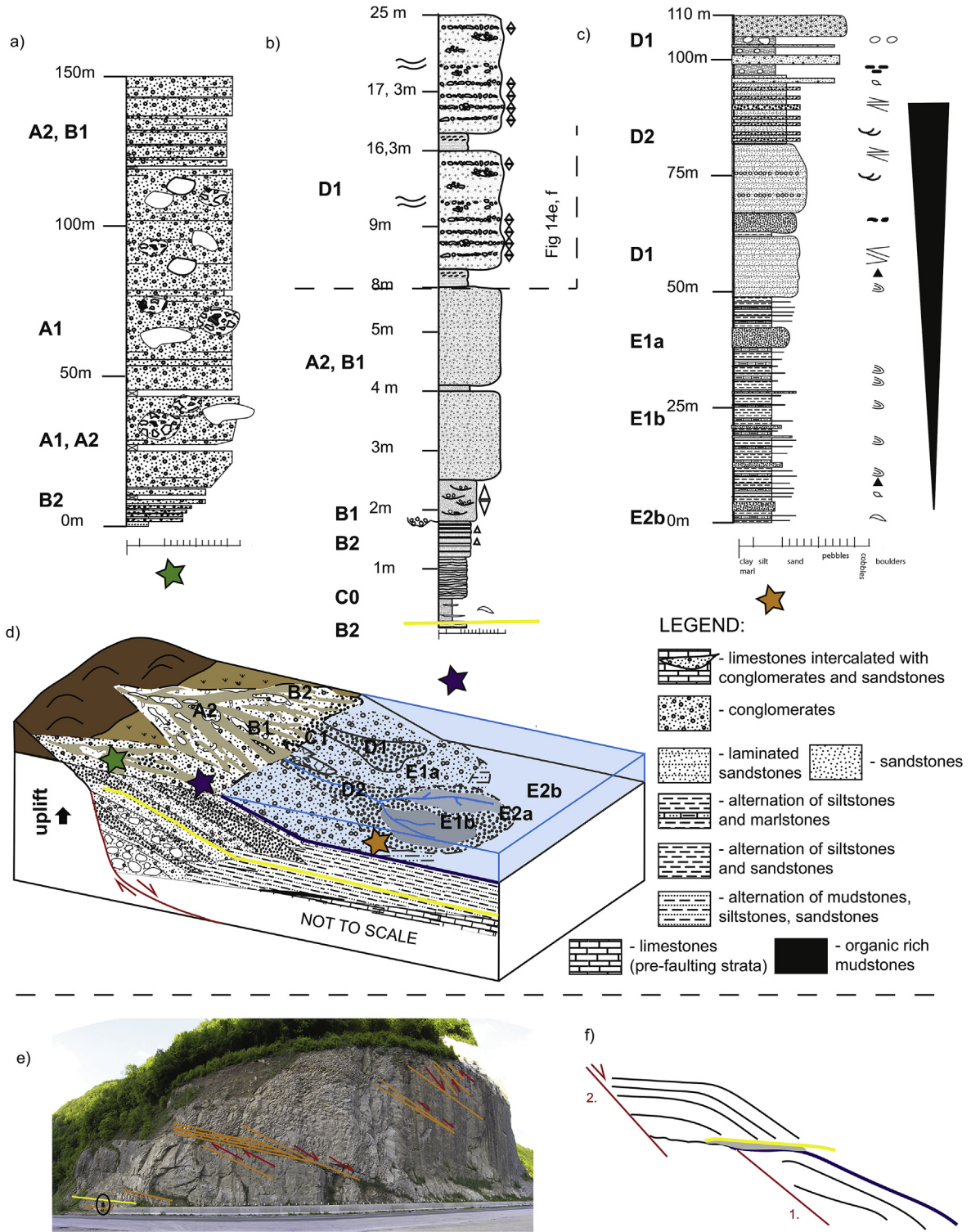
Fig. 14. Sedimentological evolution of various facies associations during low displacement rates and after faulting. a) A typical sedimentological log for the proximal part of the post-rift systems tract burying the earlier formed normal faults; b) Sedimentological log illustrating an intermediate position in the sedimentological environment around the river discharge area with coarsening upwards patterns and aggradation in the braided plain environment during normal regression (below dashed line) and progradation of delta slope deposits which are syn-kinematic to the subsequent faulting event (above dashed line). Yellow line marks the maximum flooding surface formed during highest displacement rates of the fault; c) Sedimentological log illustrating a basin-ward position in the sedimentological environment with coarsening - upwards patterns near the transition from prodelta to delta slope caused by sedimentation rate outpacing accommodation space creation rate and transport of material further into the basin; d) Interpreted sedimentological environment combining the B, C, D and E associations. Yellow line marks the maximum flooding surface developed during highest displacements rates of the fault. The dark blue line represents the maximum regressive surface; e,f) Illustration of the sedimentological response at the transition between the ceasing the activity of one fault system and initiation of the next one in its footwall. This results in a backstepping migration of the extensional deformation; e) a high frequency progradation-retrogradation pulses (red arrows) formed due to rapid changes in sedimentation rates and/or accommodation space with an overall prograding character. The yellow line marks the maximum flooding surface, the orange line delineates bedding planes. Geologists for a scale (inside black cycle); f) Interpretative sketch showing the onset of activity of next faulting event caused by the deformation migration in to footwall of the previous fault leading to drowning of previous deltaic system. The grey polygon represents transgressive system, based by the maximum regressive surface (dark blue line) and maximum flooding surface (yellow line) towards the top. The numbers 1 and 2 represent the younging trend of faulting events. See Fig. 10, Tables 1 and 2 for the meaning of facies association codes. (For interpretation of the references to colour in this figure legend, the reader is referred to the web version of this article.)
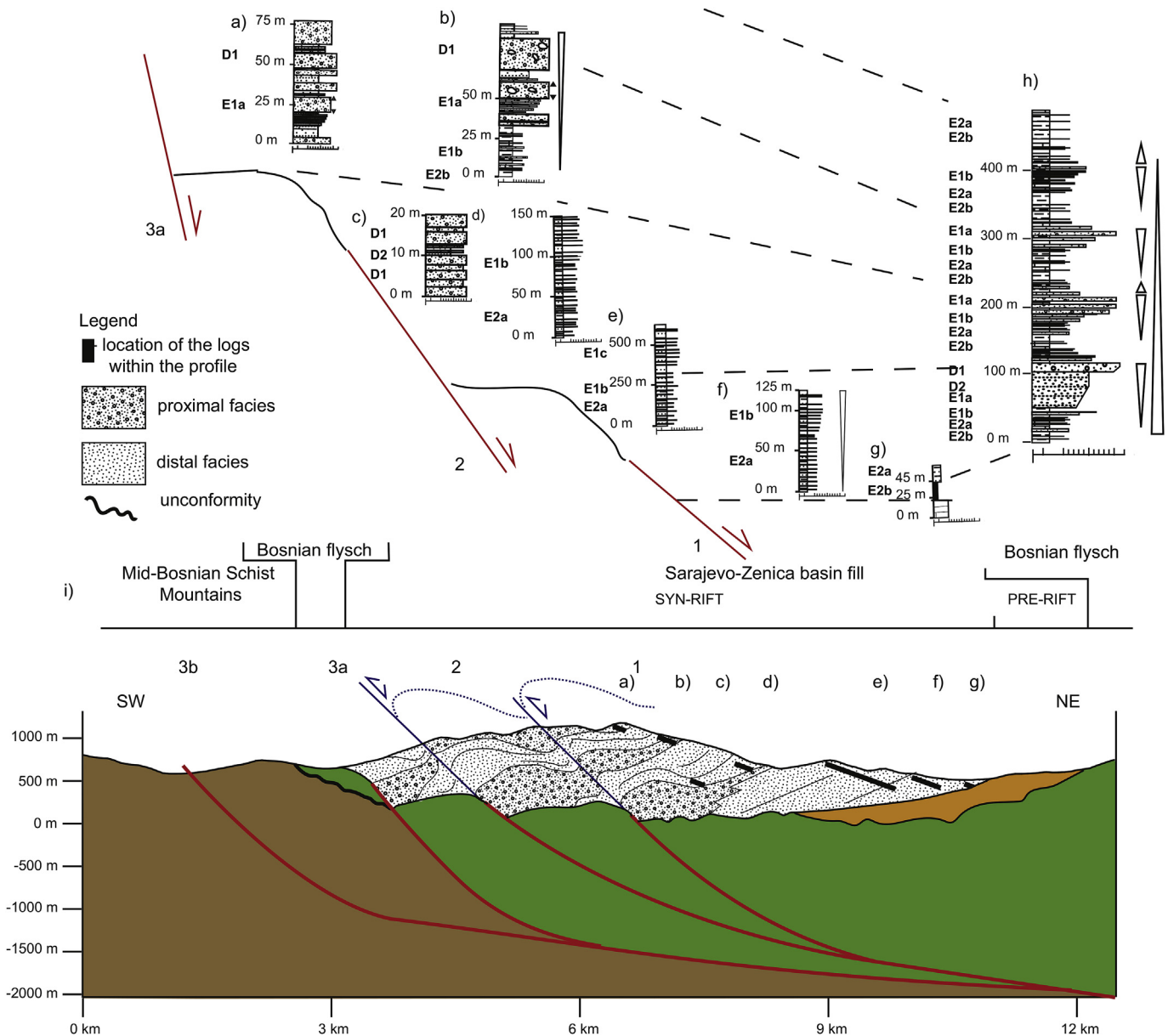
Fig. 15. An interpretative sketch of a backstepping alluvial-deltaic system following deformation migration towards the basin margin. a-g) sedimentary logs along the Hum profile; h) fining-upward cycle in the basin centre. The black dashed lines represent boundaries of the Transgressive-Regressive (T-R) cycles in column a-g. See Fig. 10 for the meaning of the facies association codes; i) Hum profile. Numbers 1, 2, 3a and 3b represent faulting events correlated with the profiles in Figs. 6 and 7. See locations in Fig. 3.

and onset of another faulting event. This cycle is controlled by the activity of a normal fault or a group of genetically related normal faults in the studied basin (Fig. 15). The thickness of such a cycle varies from 80 to 150 m as a function of the amount of accommodation space created by each event of normal faulting. In our specific studied case of the Sarajevo - Zenica basin, each normal faulting event back-stepped in the footwall and, therefore, the basin was progressively enlarged. Our analysis has detected three main transgressive-regressive cycles that are linked with the three major normal fault sets grouping the outcrop-scale faults formed during the three extensional events. These three sets are progressively younger SW-wards, i.e. in a footwall direction. The activation of the fourth set (3b in Figs. 6 and 7, i.e. the Busovača Fault stricto-senso) is associated with an incomplete developed cycle, either due to its deposition in an already filled basin with dominant proximal alluvial deposition, or due to subsequent erosion during the following post-Middle Miocene inversion of the basin. A similar

backstepping pattern of fan deposits has been documented elsewhere in the neighbouring Sava Basin of the northern Dinarides (Pavelić and Kovačić, 1999).

The higher-order cycles are bounded by sub-aerial unconformities in what was the proximal part of the basin at the time of deformation and maximum regressive surfaces in more distal parts. They have net upper boundaries. The high-order sequence boundaries are created by a renewed activation of normal faults. The migration of listric normal faulting in a footwall direction resulted in antithetic tilting of older cycles of sedimentation. The overall depositional trend of multiple cycles is retrogradation governed by the back-stepping migration of subsequent faults, whereas the proximal facies of one event is sealed by the distal facies of the next event of normal faulting (Figs. 14e, f and 15). Such a retrogradational pattern driven by progressive basin enlargement has been observed also in other extensional basins (e.g., Postma and Drinia, 1993; García-García et al., 2006).
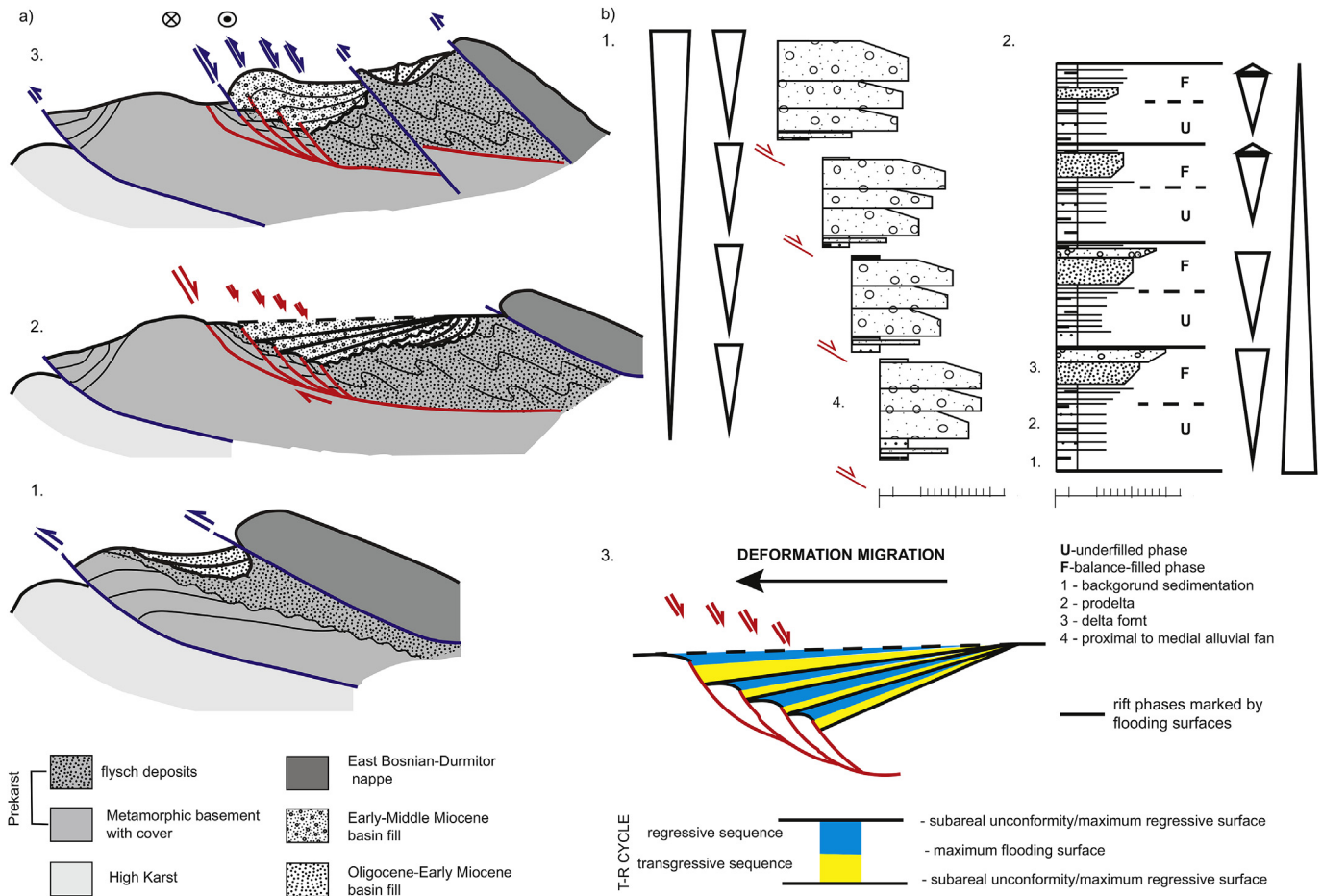
Fig. 16. a) Evolution of the Sarajevo - Zenica Basin illustrated as a conceptual model. 1 - A fordeep basin formed in front of an advancing nappe. The onset and evolution of the basin is controlled by the thrust; 2 - Tectonic inversion and formation of the asymmetric extensional basin; 3 - The final basin inversion; b) Idealized sequences of the asymmetric extensional basins. 1 - basin margin(s), showing overall coarsening - upward cycle internally arranged into smaller fining - upwards cycles; 2 - basin depocentre with overall fining - upwards cycle including of smaller coarsening - upwards cycles; 3 − T-R cyclicity induced by the backstepping migration of deformation.

The internal structure of one high-order cycle reflects the evolution of each major normal fault. The initial transgression is characterized by a fining upwards grading profile in the proximal part of basin and aggradation in more distal areas. Most of the deposition continued in alluvial environment, trapping material next to the adjacent fault scarp and cutting off supply to the distal lacustrine part of the basin (e.g., Loutit et al., 1988; Galloway, 1989). This shows that sedimentation generally kept pace with subsidence during the onset of normal faulting (Jackson et al., 2002). The onset was followed by a period of rapid subsidence in the hanging-wall of the normal fault, which was associated with aggradation and smaller scale prograding episodes. All facies associations display an overall fining upwards pattern. The short-term coarse fluxes of alluvial sediments may result in increase of the sediment supply, generally interpreted to be the result of wet climate or record of source rejuvenation due to normal fault slip (e.g., Blum, 1993). In our studied case, the latter acceleration of subsidence is rather obviously driven by the activation of normal faults. The under-filled nature of the basin during this period is a result of accommodation outpacing sediment supply due to high fault displacement rates. Similar with what was observed elsewhere (e.g., Leeder et al., 2002; Leppard and Gawthorpe, 2006), the basin is characterized by the steep, bypass and sometimes erosional slope controlled by the marginal fault and limited, narrow coastal area created by the specific geometry of the normal faults and their rapid footwall

exhumation. This stage can be generally characterized as an underfilled stage, where the rate of creating accommodation space is generally higher than the sediment supply (e.g., Carroll and Bohacs, 1999; Withjack et al., 2002). The gradual cessation of fault activity is recognized by a regression marked by rapid progradation of the delta front within the basin, creating the overall coarseningupwards grading profile. Pre-dating and on-going exhumation of normal fault footwalls increased the profile of the source area and produced high energy rivers with strong erosional character. These bedload dominated rivers carried coarse-grained material further away from the source filling up the basin and create a diachronous basal progradation surface, which is younger in a distal direction (Sweet et al., 2003; Ramaekers and Catuneanu, 2004). This stage can be generally characterized as an over-filled stage, when the rate of creating accommodation space was lower that the increased rate of sediment supply, resulting from the exhumation of the footwall (e.g. Carroll and Bohacs, 1999; Withjack et al., 2002).

At even higher resolution, the activation of faults with smaller offset observed in outcrops may be related to the definition of a higher-order cyclicity. However, such very high order cycles are difficult to discriminate from autocyclic processes, such as lateral shifting of the main channel or flooding events.

The low-order extensional cycle at the scale of the entire Lower - Middle Miocene basin fill shows an overall coarsening-upwards pattern that is superposed over the high-order transgressive-

regressive cyclicity (Figs. 15 and 16). Given the similar distribution of facies associations inside the basin, this overall coarsening-upwards pattern reflects changes in the dominant SW-ward migration of the source area. The system of normal faults gradually exhumed an increasingly active source area in their footwall (i.e. the Mid-Bosnian Schist Mountains), which increased the sediment input and filled the created accommodation space. The resulting transgressive-regressive cycles are increasingly coarser. Grading of the higher-order cycles is not always visible in the hanging-wall near the fault (e.g., Fig. 13a), whereas such grading is better documented in more distal sediments (e.g., Fig. 13b). This inference is in agreement with previous interpretations that most proximal sediments adjacent to the source area do not exhibit coarsening-upwards grading trends (e.g. Miall, 1996). Similar with what was inferred in others sedimentological studies of normal faulting (e.g., Leeder and Gawthorpe, 1987; Gawthorpe and Colella, 1990), these cycles have a wedge shape geometry due to the larger subsidence in the vicinity of normal faults.

The provenance and maturity of the material sourcing clastic wedges indicate a catchment area of the fluvial system that was dominantly located in the footwall of the normal faults (i.e. the Mid-Bosnian Schist Mountains). These are mainly local short streams sourcing small fans in the immediate hanging-wall of normal faults. Such a drainage style was observed in other extensional basins, such as the Suez Rift (Leppard and Gawthorpe, 2006), Gulf of Corinth (Gawthorpe and Leeder, 2000), or Barent Sea (Prosser, 1993). In addition to small isolated drainages, the fan systems along the Lašva and Fojnica valleys mirrors the much larger Mid-Bosnian Schists Mountains catchment area supplying large fan complex by carrying high amount of coarse material into the Sarajevo - Zenica Basin. The continuous lateral correlation between the similar deltaic succession retreating in the direction of normal faulting means that the incision kept pace with footwall uplift and maintained the sediment transport into the basin. Similar observations are available in the modern examples of Akrata and Xylokastro Deltas in Gulf of Corinth rift (e.g., Seger and Alexander, 2009). Alternatively, they can also be associated with relay ramps connecting normal fault segments (e.g. Young et al., 2000; Trudgill, 2002). We cannot fully exclude that the basin was sourced from a hanging-wall direction or by an axial drainage, but the observations of asymmetric depositional bodies show that such influxes are likely suppressed by streams with massive influx draining the footwall.

8. Tectonic and sedimentary evolution of the Sarajevo - Zenica Basin

Our study shows that sedimentation in Sarajevo-Zenica Basin during Oligocene - Miocene times was controlled dominantly by tectonically induced changes in the geometry of the accommodation space and changes in the source area. The general extensional and contractional trends in the basin have been observed or inferred also by previous studies (e.g. Hrvatović, 2006; de Leeuw et al., 2012 and references therein), but our analysis provides a much higher resolution and is able to discriminate the succession of events with time (Fig. 16), which is critical for understanding not only the tectono-sedimentary evolution of the basin, but also the larger area of the Dinarides.

8.1. Thrusting during the onset of Oligocene - Early Miocene basin deposition

Our study shows a novel demonstration that the Oligocene - Early Miocene onset of basin deposition was associated with NW-SE oriented thrusts, folds and the formation of local

unconformities during sedimentation. This NE-SW oriented contraction shows a dominantly SW tectonic transport. Grouping deformation structures and the provenance of sediments shows a direct relationship with the thrusting at a larger scale of more internal Dinarides units (East Bosnian - Durmitor and/or Drina - Ivanjica) over the basin sediments. These sediments were deposited unconformably over the Mesozoic cover of the Pre-Karst unit and over the younger, more external parts of the Bosnian Flysch (i.e. its Ugar - Durmitor Cretaceous interval). These geometries indicates that the older, more internal parts of the Bosnian Flysch (i.e. late Jurassic - Earliest Cretaceous Vranduk interval) served as a decollement horizon for the Oligocene - Early Miocene thrusting. In fact, this decollement is an inherited weakness zone from older Late Jurassic - Cretaceous thrusting that was coeval with the overall deposition of the Bosnian Flysch. In this context, the initiation of the Oligocene - Early Miocene sedimentation of the Sarajevo-Zenica basin took place in a foredeep basin that formed in the footwall of more internal Dinarides units (Fig. 16a1). At higher resolution, this Oligocene - Early Miocene sedimentation reflects likely the syn-kinematic deposition of the two sedimentary cycles described by previous studies (Muftić, 1965; Milojević, 1964). Their position in the footwall of the main thrust of more internal Dinarides units and the relative constant sediment influx infer that the cyclicity is related to two different pulses of thrusting inside the foredeep basin. This may reflect successive thrust loading and unloading events, as typically observed in many other foredeep areas (e.g., Ballato et al., 2008; Catuneanu, 2001 and references therein).

At a more regional scale, the Dinarides contraction took place during successive late Jurassic - Eocene shortening events, generally migrating towards its foreland, but also associated with moments of out-of sequence deformation (e.g., Schmid et al., 2008; Ustaszewski et al., 2010). Later, (Late) Miocene - Quaternary contractional deformations is documented by structural studies either in the external, offshore and neighbouring parts of the Dinarides or in their internal-most parts by inverting the sediments of the Pannonian Basin. The latter deformation has variable effects along the strike of the Dinarides, apparently increasing SE-wards in their external-most parts and NW-ward in the internal zone (e.g., Placer, 1999; Tomljenović and Csontos, 2001; Matenco and Radivojević, 2012; van Gelder et al., 2015 and references therein). The prolongation of contractional deformation during the Oligocene - Miocene times was quite uncertain until our study (see discussion in de Capoa et al., 1995; Mikes et al., 2008a), mostly because the bulk exhumation of the Dinarides took place earlier, combined with similar contractional directions and uncertainties in dating the Miocene sediments in the intra-montane basins. Therefore, our study is a first clear demonstration of a link between contraction and sedimentation that post-dated the main Eocene event in the central part of the Dinarides. Although affected by age uncertainties, the syn-kinematic Oligocene - Early Miocene sediments that document this contraction must predate the ~18 Ma onset of deposition of the second cycle representing the initiation of the Dinaride Lake System and the start of the main extensional phase in the Pannonian Basin (de Leeuw et al., 2012; Mandic et al., 2012). Although the Late Oligocene Climatic Optimum that stalled in the Aquitanian may have imprinted the sedimentation of the Dinaride Lake System (de Leeuw et al., 2012), the coeval first depositional cycle in the Sarajevo – Zenica Basin was primarily controlled by tectonics.

8.2. Early - Middle Miocene extension

The earlier contraction was followed in the Sarajevo-Zenica Basin by the deposition of a new low-order tectono - sedimentary

cycle. This extensional deposition is slightly shifted SW-wards in respect to the earlier tectono-sedimentary cycle by directly over-lying the pre-Oligocene basement and sedimentary cover of the Pre-Karst unit (Fig. 16a2). The overall NE-SW to E-W direction of extension has local variations during the successive normal faulting events. The geometry of the normal faults and the antithetic tilting of their hanging-walls indicate that the four major listric normal faults merge at depth into one major decollement level (Figs. 6, 7, 15 and 16b) that is rooted somewhere in the Bosnian Flysch, most likely in its younger Ugar - Durmitor component. Once again, the presence of this decollement horizon located at the contact be-tween the basement and dominantly carbonatic cover of the pre-Karst and East Bosnian − Durmitor units has facilitated its reac-tivation by the NE-SW oriented extension.

The coeval exhumation of the Mid-Bosnian Schists Mountains located in the footwall of the normal fault system is inferred by eroded footwalls and the geometry of these faults. Exhumation studies in the Mid-Bosnian Schist Mountains show a few late Miocene − early Pliocene apatite U-Th/He ages (5−7 Ma) in the immediate footwall of the Busovača Fault, while zircon fission fission-tracks are generally older than 27−28 Ma in the Mid-Bosnian Schists Mountains (Casale, 2012). A more recent study derived zircon fission track ages of 24−29 Ma in the immediate footwall of the main Busovača fault (Hrvatović et al., 2015). This means that zircon fission track and higher temperature thermo-chronological Eocene-Oligocene and older ages must reflect also the first stage of contraction observed also in the Sarajevo-Zenica Basin. The Late Miocene - Pliocene lower temperature thermo-chronological ages reflect exhumation coeval with the last observed stage of contraction. The ages predate and post-date with a few million years the main Early - Middle extensional basin for-mation. Given the partial retention zones of zircon and apatite fisson track and U-Th/He, this limits the Mid-Bosnian Schist Mountains exhumation during the Early - Middle Miocene exten-sion somewhere between 3 and 5 km at normal geothermal gra-dients. The Busovača fault system reflects the brittle deformation associated with this exhumation. Therefore, we conclude that this represents an uni-directional low-angle listric normal fault system that is associated with footwall exhumation. Obviously, this asymmetry is facilitated by pre-existence of the rheological weak-ness of the Bosnian Flysch.

The extensional depositional cycle observed in the Sarajevo-Zenica Basin is regionally coeval with the initiation of the Dinar-ide Lake System. The lacustrine phase took place from 18 to ~13 Ma (de Leeuw et al., 2012), culminating at ~15.5 Ma when the lake system gained its maximum extent, interpreted to be an effect of favourable conditions during the Miocene Climatic Optimum (Zachos et al., 2001). The coeval evolution of the Sarajevo-Zenica Basin was almost entirely controlled by the extension. The Miocene Climatic Optimum might have enhanced the favourable conditions of extending the lake, but its subsidence is certainly tectonically controlled. At a more regional scale, this phase of extension was coeval with the overall Miocene extension that started at ~20−18 Ma in the main depocentres of the Pannonian Basin. The northern margin of the Dinarides adjacent to the Pan-nonian Basin was affected by coeval large scale extensional exhu-mation along detachments that indicate top-N to top-E extension along the Dinarides strike. This extension peaked ~15−11 Ma and its onset is generally older in the eastern areas of Serbia, such as Fruška Gora or the Morava corridor (Ustaszewski et al., 2010; Stojadinović et al., 2013; Toljić et al., 2013; van Gelder et al., 2015). Closer to our studied area, Miocene extension affected also the internal units of the Dinarides (Ilić and Neubauer, 2005; Schefer et al., 2011). This overall extension resulted in the formation of asymmetric extensional basins, where the hanging-wall

subsidence was associated with significant exhumation in the footwall of detachments or normal faults (e.g., Matenco and Radivojević, 2012). These studies have shown that the location of these detachments is controlled by the weakness of various inherited Dinarides nappe contacts, most often made up by contractional trench turbidites. This is strikingly similar with the Sarajevo - Zenica Basin, whose Early - Middle Miocene normal faulting was associated with footwall exhumation of the Mid-Bosnian Schist Mountains was controlled by the inherited weak-ness of the Bosnian Flysch unit. Therefore, the observed extension must have the same genetic cause. The Sarajevo - Zenica Basin is the most external area in the Dinarides documented so far by a field study to be affected by the extension of the Pannonian Basin.

8.3. Late Miocene and subsequent inversion

The overall basin fill was inverted by a post-Middle Miocene stage of contractional deformation that was observed in many other areas of the Dinarides (Tomljenović and Csontos, 2001; Ustaszewski et al., 2014 and references therein) and is likely still active at present (Bennett et al., 2008). In our studied case of the Sarajevo - Zenica Basin, the basin was inverted with a N-S oriented direction of contraction (Fig. 16a3). The obliquity of this inversion direction to the NW-SE oriented structural grain of the inherited normal fault system resulted in the inversion of this system over oblique ramps associated with a large number of tear and transfer faults. It is rather clear that the distribution of sedimentological facies from coarse alluvial in the SW to more distal turbiditic to pelagic in the NE inherited from extensional phases controlled the geometry of the subsequent contractional deformation. The resul-ted geometry is the one of en-echelon thrusts and folds accom-modated by transfer zones or tear faults. Most of the deformation has a S-ward vergence, but opposite N-verging back-thrusts or folds are also observed, although accommodating lower amounts of shortening. Unsurprisingly, their prolongation at depth appears to be connected at depth into a larger offset decollement that is rooted, yet again, in the Bosnian Flysch thrust contact. In the SW parts of the Sarajevo-Zenica basin (Figs. 1 and 3), coeval deposition in several synforms suggests that sedimentation took place in for-deep basins, although sedimentological patterns, dominated by alluvial and other continental sub-aerial deposition, are not fully diagnostic. The deposition in the basin was also associated or post-dated by the final contractional exhumation of the Mid-Bosnian Schist Mountains, as documented by the apatite U-Th/He low temperature thermochronology data (~5−7 Ma, Casale, 2012).

9. Conclusions

Our study of the Sarajavo - Zenica Basin, a large isolated Oligo-cene - Miocene basin situated in the centre of the Dinarides orogen, has demonstrated a novel succession of deformation events, with critical inferences for the evolution of this mountain chain, and serves as a quantitative example of analysing the link between normal faulting and sedimentological evolution in asymmetric extensional basins.

The Oligocene - Early Miocene contraction was responsible for the onset of deposition in a basin that formed as a foredeep in the footwall of the coeval thrust displacing more internal Dinarides units over the Pre-Karst nappe situated in its footwall, and reactivating the inherited Bosnian Flysch Late Jurassic - Cretaceous tectonic contact. This thrusting has resulted in the creation of two transgressive-regressive cycles that reflect pulses of deformation during the overall contraction. At regional scale, this observation solves a long-standing controversy and shows that contractional deformation continued during Oligocene - Early Miocene times after the main

Late Eocene orogenic phase in the central part of the Dinarides. More precise dating of this cycle of deposition is required for an accurate age determination of this deformation. The contraction was subsequently followed by a new cycle of deposition in the basin driven by the activation of a system of NE-dipping normal faults and the creation of an asymmetric extensional basin associated with significant exhumation in the SW-ward located footwall of normal faults. Deformation migrated towards this footwall with time, enlarging the basin and creating the space for the repetition of a higher order transgressive-regressive cyclicity observed in the alluvial to deep water turbiditic and pelagic coeval depositional system. At a larger scale, the observation of this extensional evolution proves that the extension of the Pannonian Basin was felt much further SW-wards than previously thought, re-activating thrust contacts inherited from the previous contractional evolution. The basin was affected ultimately by the overall indentation of Adriatic units and inversion observed in more internal units, a process that continued and is active today in most of the Dinarides (e.g., Pinter et al., 2005; Bennett et al., 2008; Handy et al., 2010).

The Early - Middle Miocene basin fill and extensional kinematics serve as a very good example of understanding systems tracts in asymmetric extensional basin. Our analysis demonstrates that the first order pattern of basin fill is regressive, coarsening-upwards, driven by the increasing and coeval exhumation during extension of a source area situated in the footwall of the normal faults, i.e. the Mid-Bosnian Schist Mountains. This gradually growing source area ensured an almost uni-directional sourcing of the basin and a marked asymmetry of the distribution of the sedimentological facies inside the basin, that is almost exclusively coarse grained alluvial to deltaic fan in the SW and more distal in the NE. Over this overall first order pattern (or low order cycle), a higher order cyclicity grouping transgressive and regressive systems tracts is observed to be directly associated with the activity of individual normal faults. These cycles have characteristic sedimentological patterns during the onset, maximum rate of slip along normal faults and their gradual ceasing, from alluvial facies and wedges in proximal parts of normal faults to deeper water deposition at higher distances in their footwall. Sequence boundaries are formed during moments when the normal faults migrate further in a footwall direction and created a drowning of pre-existing alluvial fans and proximal deltaic facies and their shift in the same direction. Increasing the source area by footwall exhumation results in a massive SW-ward sourcing that ultimately fills the basin completely at very high rates during the final regression.

The overall analysis of such extensional basins shows that asymmetry and footwall exhumation changes significantly the sequence stratigraphy of extensional systems, which is almost exclusively studied so far in basins buried beneath passive continental margins (e.g., Martins-Neto and Catuneanu, 2010 and references therein). It shows that sedimentation in asymmetric basins, often observed in back-arc or intra-montane areas, is dominantly controlled rheologically by the inherited weakness of pre-existing nappe contacts (e.g., Tari et al., 1992; Brun and Faccenna, 2008). The asymmetric depositional geometry is imprinted in the high resolution transgressive-regressive cycles. The source input increases by footwall exhumation until the basin is completely filled during the rapid extension. Such basins deserve further studies and a better expression in current research of depositional characteristics in active tectonic settings.

Acknowledgements

References

Aubouin, J., Blanchet, R., Cadet, J.-P., Celet, P., Charvet, J., Chorowicz, J., Cousin, M., Rampnoux, J.-P., 1970. Essai sur la géologie des Dinarides. Bull. Soc. Géol. Fr. 12, 1060–1095.

Balázs, A., Matenco, L., Magyar, I., Horváth, F., Cloetingh, S., 2016. The link between tectonics and sedimentation in back-arc basins: new genetic constraints from the analysis of the Pannonian Basin. Tectonics 35, 1526–1559.

Ballato, P., Nowaczyk, N.R., Landgraf, A., Strecker, M.R., Friedrich, A., Tabatabaei, S.H., 2008. Tectonic control on sedimentary facies pattern and sediment accumulation rates in the Miocene foreland basin of the southern Alborz Mountains, northern Iran. Tectonics 27, TC6001.

Bargnesi, E.A., Stockli, D.F., Mancktelow, N., Soukis, K., 2013. Miocene core complex development and coeval supradetachment basin evolution of Paros, Greece, insights from (U–Th)/He thermochronometry. Tectonophysics 595–596, 165–182.

Bennett, R.A., Hreinsdóttir, S., Buble, G., Bašic, T., Bačić, Ž., Marjanović, M., Casale, G., Gendaszek, A., Cowan, D., 2008. Eocene to present subduction of southern Adria mantle lithosphere beneath the Dinarides. Geology 36, 3–6.

Benvenuti, M., Bertini, A., Conti, C., Dominici, S., 2007. Integrated analyses of litho- and biofacies in a Pliocene cyclothemic, alluvial to shallow marine succession (Tuscany, Italy). Geobios 40 (2), 143–158.

Bertotti, G., Podladchikov, Y., Daehler, A., 2000. Dynamic link between the level of ductile crustal flow and style of normal faulting of brittle crust. Tectonophysics 320, 195–218.

Blum, M.D., 1993. Genesis and Architecture of Incised Valley Fill Sequences: a Late Quaternary Example from the Colorado River. Gulf Coastal Plain of Texas: (Chapter 10): Recent Applications of Siliciclastic Sequence Stratigraphy.

Bouma, A.H., Kuenen, P.H., Shepard, F.P., 1962. Sedimentology of Some Flysch Deposits: a Graphic Approach to Facies Interpretation, vol. 168. Elsevier, Amsterdam.

Brun, J.-P., Faccenna, C., 2008. Exhumation of high-pressure rocks driven by slab rollback. Earth Planet. Sci. Lett. 272, 1–7.

Cao, S., Neubauer, F., Bernroider, M., Liu, J., Genser, J., 2013. Structures, microfabrics and textures of the Cordilleran-type Rechnitz metamorphic core complex. East. Alps. Tectonophys. 608, 1201–1225.

Carroll, A.R., Bohacs, K.M., 1999. Stratigraphic classification of ancient lakes: balancing tectonic and climatic controls. Geology 27 (2), 99–102.

Casale, G.M., 2012. Core Complex Exhumation in Peri-Adriatic Extension and Kinematics of Neogene Slip along the Saddle Mountains Thrust. University of Washington, p. 93.

Catuneanu, O., 2001. Flexural partitioning of the late archaean witwatersrand foreland system, South Africa. Sediment. Geol. 141, 95–112.

Catuneanu, O., 2002. Sequence stratigraphy of clastic systems: concepts, merits, and pitfalls. J. Afr. Earth Sci. 35, 1–43.

Cloetingh, S., Haq, B.U., 2015. Inherited landscapes and sea level change. Science 347, 1258375.

Colella, A., 1988. Pliocene-Holocene fan deltas and braid deltas in the Crati Basin, southern Italy: a consequence of varying tectonic conditions. In: Fan deltas: Sedimentology and Tectonic Settings, 152, pp. 50–74.

de Capoa, P., Radoičić, R., D'Argenio, B., 1995. Late Miocene deformation of the external Dinarides (Montenegro and dalmatia). New biostratigraphic evidence. Mem.Sci. Geol. 47, 157–172.

de Leeuw, A., Mandic, O., Vranjković, A., Pavelić, D., Harzhauser, M., Krijgsman, W., Kuiper, K.F., 2010. Chronology and integrated stratigraphy of the Miocene sinj basin (Dinaride Lake system, Croatia). Palaeogeogr. Palaeoclimatol. Palaeoecol. 292, 155–167.

de Leeuw, A., Mandic, O., Krijgsman, W., Kuiper, K., Hrvatović, H., 2012. Paleomagnetic and geochronologic constraints on the geodynamic evolution of the Central Dinarides. Tectonophysics 530–531, 286–298.

DeCelles, P.G., Gray, M.B., Ridgway, K.D., Cole, R.B., Pivnik, D.A., Pequera, N., Srivastava, P., 1991. Controls on synorogenic alluvial-fan architecture, beartooth conglomerate (palaeocene). Wyo. Montana. Sedimentol. 38 (4), 567–590.

Delvaux, D., Sperner, B., 2003. Stress tensor inversion from fault kinematic indicators and focal mechanism data: the TENSOR program. In: Nieuwland, D. (Ed.), New Insights into Structural Interpretation and Modelling. Geological Society, London.

Dimitrijević, M.D., 1997. Geology of Yugoslavia, second ed. Geoinstitute, Belgrade,

Belgrade.

Dimitrijević, M.N., Dimitrijević, M.D., 1987. The Turbiditic Basins of Serbia. Serbian Academy of Sciences and Arts Department of Natural & Mathematical Sciences.

Dimitrijević, M.N., Dimitrijević, M.D., 1991. Triassic carbonate platform of the Drina-Ivanjica element (Dinarides). Acta Geol. Hung. 34, 15—44.

Embry, A., Johannessen, E., 1992. T—R sequence stratigraphy, facies analysis and reservoir distribution in the uppermost Triassic—Lower Jurassic succession, Western Sverdrup Basin, Arctic Canada. In: Arctic Geology and Petroleum Potential, Special Publication, 2, pp. 121—146.

Faccenna, C., Piromallo, C., Crespo-Blanc, A., Jolivet, L., Rosetti, F., 2004. Lateral slab deformation and the origin of the western Mediterranean arcs. Tectonics 23, TC1012, 1010.1029/2002TC001488.

Fodor, L., Csontos, L., Bada, G., Györfi, I., Benkovics, L., 1999. Tertiary tectonic evolution of the Pannonian basin system and neighbouring orogens: a new synthesis of paleostress data. In: Durand, B., Jolivet, L., Horvath, F., Seranne, M. (Eds.), The Mediteranean Basins: Tertiary Extension within the Alpine Orogen. The Geological Society, London, pp. 295—334.

Friedmann, S.J., Burbank, D.W., 1995. Rift basins and supradetachment basins: intracontinental extensional end-members. Basin Res. 7 (2), 109—127.

Galloway, W.E., 1989. Calstic facies models, depositional systems, sequences and correlation: a sedimentologists view of the dimensional and temporal resolution of lithostratigraphy. In: Cross, T.A. (Ed.), Quantitative Dynamic Stratigraphy. Prentice Hall, New Jersey, pp. 113—126.

Garcia-Castellanos, D., Verges, J., Gaspar-Escribano, J., Cloetingh, S., 2003. Interplay between tectonics, climate, and fluvial transport during the Cenozoic evolution of the Ebro Basin (NE Iberia). J. Geophys. Res. 108, 2347, 2310.1029/2002JB002073.

García-García, F., Fernández, J., Viseras, C., Soria, J.M., 2006. Architecture and sedimentary facies evolution in a delta stack controlled by fault growth. Sediment. Geol. 185, 79—92.

Gawthorpe, R.L., Colella, A., 1990. Tectonic Controls on Coarse-grained Delta Depositional Systems in Rift Basins. Systems in Rift Basins, vol. 27. Special Publication 10 of the IAS, Coarse-Grained Deltas, p. 113.

Gawthorpe, R.L., Leeder, M.R., 2000. Tectono-sedimentary evolution of active extensional basins. Basin Res. 12, 195—218.

Handy, M.R.M., Schmid, S., Bousquet, R., Kissling, E., Bernoulli, D., 2010. Reconciling plate-tectonic reconstructions of Alpine Tethys with the geological-geophysical record of spreading and subduction in the Alps. Earth Sci. Rev. 102, 121—158.

Handy, M.R., Ustaszewski, K., Kissling, E., 2015. Reconstructing the Alps—Carpathians—Dinarides as a key to understanding switches in subduction polarity, slab gaps and surface motion. Int. J. Earth Sci. 104 (1), 1—26.

Harzhauser, M., Mandic, O., 2008. Neogene lake systems of Central and South-Eastern Europe: faunal diversity, gradients and interrelations. Paleogeogr. Paleoclimatol. Paleoecol. 260, 417—434.

Helland-Hansen, W., Martinsen, O.J., 1996. Shoreline trajectories and sequences: description of variable depositional-dip scenarios. J. Sediment. Res. 66 (4), 670—688.

Herak, D., Herak, M., Tomljenović, B., 2009. Seismicity and earthquake focal mechanisms in North-Western Croatia. Tectonophysics 465, 212—220.

Hinsken, S., Ustaszewski, K., Wetzel, A., 2007. Graben width controlling syn-rift sedimentation: the Palaeogene southern Upper Rhine Graben as an example. Int. J. Earth Sci. 96, 979—1002.

Horváth, F., Musitz, B., Balázs, A., Végh, A., Uhrin, A., Nádor, A., Koroknai, B., Pap, N., Tóth, T., Wórum, G., 2015. Evolution of the Pannonian basin and its geothermal resources. Geothermics 53, 328—352.

Hrvatović, H., 2006. Geological Guidebook through Bosnia and Herzegovina. Geological Survey of Federation Bosnia and Herzegovina, Sarajevo.

Hrvatović, H., Pamić, J., 2005. Principal thrust-nappe structures of the Dinarides. Acta Geol. Hung. 48/2, 133—151.

Hrvatović, H., Dunkl, I., Strmić-Palinkaš, S., Palinkaš, L., 2015. A new research results metamorphic complex of the Mid-Bosnian Schist Mountains. I Kongres geologa u Bosni i Hercegovini sa međunarodnim učešćem, Zbornik radova, 127—132. Udruženje geologa Bosne i Hercegovine, ISSN 1840-4073, Tuzla, 21-23.10.2015.

Ielpi, A., 2012. Anatomy of major coal successions: facies analysis and sequence architecture of a brown coal-bearing valley fill to lacustrine tract (Upper Valdarno Basin, Northern Apennines, Italy). Sediment. Geol. 265, 163—181.

Ilić, A., Neubauer, F., 2005. Tertiary to recent oblique convergence and wrenching of the Central Dinarides: constraints from a palaeostress study. Tectonophysics 410, 465—484.

Jackson, C.A.L., Gawthorpe, R.L., Sharp, I.R., 2002. Growth and linkage of the East Tanka fault zone, Suez rift: structural style and syn-rift stratigraphic response. J. Geol. Soc. 159 (2), 175—187.

Jackson, C.A.L., Gawthorpe, R.L., Carr, I.D., Sharp, I.R., 2005. Normal faulting as a control on the stratigraphic development of shallow marine syn-rift sequences: the Nukhul and Lower Rudeis Formations, Hammam Faraun fault block, Suez Rift, Egypt. Sedimentology 52 (2), 313—338.

Jiménez-Moreno, G., de Leeuw, A., Mandic, O., Harzhauser, M., Pavelić, D., Krijgsman, W., Vranjkovic, A., 2009. Integrated stratigraphy of the early Miocene lacustrine deposits of pag Island (SW Croatia): palaeovegetation and environmental changes in the Dinaride Lake system. Palaeogeogr. Palaeoclimatol. Paleoecol. 280, 193—206.

Jolivet, L., Brun, J.-P., 2010. Cenozoic geodynamic evolution of the Aegean. Int. J. Earth Sci. 99, 109—138.

Jolivet, L., Faccenna, C., 2000. Mediterranean extension and the Africa-Eurasia collision. Tectonics 19, 1095—1106.

Jovanović, R., Mojićević, M., Tokić, S., Rokić, Lj, 1971. Basic Geological Map of the SFRY, 1:100.000, Sheet Sarajevo (K-34I). Federal Geological Institute, Belgrade.

Korbar, T., 2009. Orogenic evolution of the external Dinarides in the NE adriatic region: a model constrained by tectonostratigraphy of upper cretaceous to Paleogene carbonates. Earth Sci. Rev. 96, 296—312.

Krstić, N., Savić, L., Jovanović, G., Bodor, E., 2003. Lower Miocene lakes of the balkan land. Acta Geol. Hung. 46/3, 291—299.

Leeder, M., Collier, R., Abdul Aziz, L., Trout, M., Ferentinos, G., Papatheodorou, G., Lyberis, E., 2002. Tectono-sedimentary processes along an active marine/lacustrine half-graben margin: Alkyonides Gulf, E. Gulf of Corinth, Greece. Basin Res. 14, 25—41.

Leeder, M.R., Gawthorpe, R.L., 1987. Sedimentary Models for Extensional Tilt-block/half-graben Basins, vol. 28. Geological Society, London, pp. 139—152. Special Publications (1).

Leever, K.A., Matenco, L., Garcia-Castellanos, D., Cloetingh, S.A.P.L., 2011. The evolution of the Danube gateway between Central and Eastern Paratethys (SE Europe): insight from numerical modelling of the causes and effects of connectivity between basins and its expression in the sedimentary record. Tectonophysics 502, 175—195.

Leppard, C.W., Gawthorpe, R.L., 2006. Sedimentology of rift climax deep water systems; lower Rudeis formation, Hammam Faraun fault block, Suez Rift, Egypt. Sediment. Geol. 191 (1), 67—87.

Lister, G.S., Davis, G.A., 1989. The origin of metamorphic core complexes and detachment faults formed during tertiary continental extension in the northern Colorado river region, USA. J. Struct. Geol. 11, 65—94.

Longhitano, S.G., Sabato, L., Tropeano, M., Murru, M., Carannante, G., Simone, L., Cilona, A., Vigorito, M., 2015. Outcrop reservoir analogous and porosity changes in continental deposits from an extensional basin: the case study of the upper Oligocene Sardinia Graben System, Italy. Mar. Pet. Geol. 67, 439—459.

Loutit, T.S., Hardenbol, J., Vail, P.R., Baum, G.R., 1988. Condensed sections: the key to age-dating and correlation of continental margin sequences. In: Wilgus, C.K., Hastings, B.S., Kendall, C. G. St. C., Posamentier, H.W., Ross, C.A., Van Wagoner, J.C. (Eds.), Sea Level Changes—an Integrated Approach, vol. 42. SEPM Special Publication, pp. 183—213.

Lowe, D.R., 1982. Sediment gravity flows: II Depositional models with special reference to the deposits of high-density turbidity currents. J. Sediment. Res. 52 (1), 279—297.

Mandic, O., de Leeuw, A., Vuković, B., Krijgsman, W., Harzhauser, M., Kuiper, K.F., 2011. Palaeoenvironmental evolution of lake Gacko (southern Bosnia and Herzegovina): impact of the middle Miocene climatic Optimum on the Dinaride Lake system. Palaeogeogr. Palaeoclimatol. Palaeoecol. 299, 475—492.

Mandic, O., de Leeuw, A., Bulić, J., Kuiper, K., Krijgsman, W., Jurišić-Polšak, Z., 2012. Paleogeographic evolution of the Southern Pannonian Basin: 40Ar/39Ar age constraints on the Miocene continental series of northern Croatia. Int. J. Earth Sci. 101, 1033—1046.

Martín-Barajas, A., Vázquez-Hernández, S., Carreño, A.L., Helenes, J., Suárez-Vidal, F., Alvarez-Rosales, J., 2001. Late Neogene stratigraphy and tectonic control on facies evolution in the Laguna Salada Basin, northern Baja California, Mexico. Sediment. Geol. 144, 5—35.

Martins-Neto, M.A., Catuneanu, O., 2010. Rift sequence stratigraphy. Mar. Petroleum Geol. 27, 247—253.

Matenco, L., Radivojević, D., 2012. On the formation and evolution of the Pannonian Basin: constraints derived from the structure of the junction area between the Carpathians and Dinarides. Tectonics 31, TC6007.

Melchor, R.N., 2007. Changing lake dynamics and sequence stratigraphy of synrift lacustrine strata in a half-graben: an example from the Triassic Ischigualasto—Villa Unión Basin, Argentina. Sedimentology 54 (6), 1417—1446.

Miall, A.D., 1985. Architectural-element Analysis: a New Method of Facies Analysis Applied to Fluvial Deposits.

Miall, A.D., 1996. The Geology of Fluvial Deposits. Springer, New York, p. 582.

Miall, A.D., Miall, C.E., 2001. Sequence stratigraphy as a scientific enterprise: the evolution and persistence of conflicting paradigms. Earth Sci. Rev. 54, 321—348.

Mikes, T., Báldi-Beke, M., Kázmér, M., Dunkl, I., von Eynatten, H., 2008a. Calcareous Nannofossil Age Constraints on Miocene Flysch Sedimentation in the Outer Dinarides (Slovenia, Croatia, Bosnia-herzegovina and Montenegro), vol. 298. Geological Society, London, pp. 335—363. Special Publications.

Mikes, T., Christ, D., Petri, R., Dunkl, I., Frei, D., Báldi-Beke, M., Reitner, J., Wemmer, K., Hrvatović, H., von Eynatten, H., 2008b. Provenance of the bosnian flysch. Swiss J. Geosci. 101, 31—54.

Milojević, R., 1964. Geologic Composition and Tectonic Pattern of Middle-bosnia Coal Basin with Special Review of Development and Economic Value of Coal-bearing Facies. PhD Thesis. Geological survey Sarajevo special publication, p. 190.

Muftić, M., 1965. Geological Relationship between Coal Terrains between Mid-Bosnian Coal Mines. Geološki glasnik, Geological survey Sarajevo special publication, Bila, Zenica, Kakanj and Breza, p. 108.

Mulder, T., Alexander, J., 2001. Abrupt change in slope causes variation in the deposit thickness of concentrated particle-driven density currents. Mar. Geol. 175 (1), 221—235.

Nemec, W., Postma, G., 1993. Quaternary alluvial fans in southwestern Crete: sedimentation processes and geomorphic evolution. In: In Alluvial Sedimentation, vol. 17. IAS Special Publication, pp. 235—276.

Nemec, W., Steel, R., 1984. Alluvial and Coastal Conglomerates: Their Significant Features and Some Comments on Gravelly Mass-flow Deposits.

Nottvedt, A., Gabrielsen, R.H., Steel, R.J., 1995. Tectonostratigraphy and sedimentary

architecture of rift basins, with reference to the northern North Sea. Mar. Pet. Geol. 12, 881–901.

Olujić, J., Pamić, J., Pamić, O., Milojević, R., Veljković, D., Kapeler, I., 1978. Basic Geological Map of the SFRY, 1:100.000, Sheet Vareš (L-34-133). Federal Geological Institute, Belgrade.

Pamić, J., 2002. The sava-vardar zone of the Dinarides and hellenides versus the Vardar Ocean. Eclogae Geol. Helv. 95, 99–113.

Pamić, J., Balogh, K., Hrvatović, H., Balen, D., Jurković, I., Palinkaš, L., 2004. K–Ar and Ar–Ar dating of the palaeozoic metamorphic complex from the Mid-Bosnian Schist Mts., central Dinarides, Bosnia and Hercegovina. Min. Pet. 82, 65–79.

Pavelić, D., Kovačić, M., 1999. Lower Miocene alluvial deposits of the pozeska Mt. (Pannonian Basin, northern Croatia): cycles, megacycles and tectonic implications. Geol. Croat. 52 (1), 67–76.

Pedrera, A., Galindo-Zaldìvar, J.s., Lamas, F., Ruiz-Const·n, A., 2012. Evolution of near-surface ramp-flat-ramp normal faults and implication during intramontane basin formation in the eastern Betic Cordillera (the Huercal-Overa Basin, SE Spain). Tectonics 31, TC4024.

Pinter, N., Grenerczy, G., Weber, J., Stein, S., Medak, D., 2005. The Adria Microplate: GPS Geodesy, Tectonics and Hazards (Nato Science Series: IV: Earth and Environmental Sciences). Springer, p. 413.

Placer, L., 1999. Contribution to the macrotectonic subdivision of the border region between southern Alps and external Dinarides. Geologija 41, 223–255.

Posamentier, H.W., Allen, G.P., 1993. Variability of the sequence stratigraphic model: effects of local basin factors. Sediment. Geol. 86, 91–109.

Postma, G., 1984. Slumps and their deposits in fan delta front and slope. Geology 12 (1), 27–30.

Postma, G., 1990. An analysis of the variation in delta architecture. Terra nova. 2 (2), 124–130.

Postma, G., Drinia, H., 1993. Architecture and sedimentary facies evolution of a marine, expanding outer-arc half-graben (Crete, late Miocene). Basin Res. 5 (2), 103–124.

Prior, D.B., Bornhold, B.D., 1988. Submarine Morphology and Processes of Fjord Fan Deltas and Related High-gradient Systems: Modern Examples from British Columbia. sedimentology and tectonic settings, Fan deltas, pp. 125–143.

Prosser, S., 1993. Rift-related Linked Depositional Systems and Their Seismic Expression, vol. 71. Geological Society, London, pp. 35–66. Special Publications (1).

Răbăgia, T., Matenco, L., Cloetingh, S., 2011. The interplay between eustasy, tectonics and surface processes during the growth of a fault-related structure as derived from sequence stratigraphy: the Govora–Ocnele Mari antiform, South Carpathians. Tectonophysics 502, 196–220.

Ramaekers, P., Catuneanu, O., 2004. Development and sequences of the athabasca basin, early proterozoic, saskatchewan and alberta, Canada. The precambrian Earth: tempos and events. Dev. Precambrian Geol. 12, 705–723.

Rampnoux, J.P., 1970. Regards sur les Dinarides internes yougoslaves (Serbie-Monténégro oriental): stratigraphie, évolution paléogéographique, magmatisme. Bull. Soc. Géol. Fr. 12, 948–966.

Ratschbacher, L., Frisch, W., Linzer, H.G., Merle, O., 1991. Lateral extrusion in the eastern Alps; Part 2, structural analysis. Tectonics 10, 257–271.

Robertson, A.H.F., 2011. Late Palaeozoic - cenozoic tectonic development of Greece and Albania in the context of alternative reconstructions of Tethys in the Eastern Mediterranean region. Int. Geol. Rev. 54, 373–454.

Rosenbaum, G., Regenauer-Lieb, K., Weinberg, R., 2005. Continental extension: from core complexes to rigid block faulting. Geology 33, 609–612.

Schefer, S., Cvetković, V., Fügenschuh, B., Kounov, A., Ovtcharova, M., Schaltegger, U., Schmid, S., 2011. Cenozoic granitoids in the Dinarides of southern Serbia: age of intrusion, isotope geochemistry, exhumation history and significance for the geodynamic evolution of the Balkan Peninsula. Int. J. Earth Sci. 100, 1181–1206.

Schlager, W., 1993. Accommodation and supply - a dual control on stratigraphic sequences. Sediment. Geol. 86, 111–136.

Schmid, S., Bernoulli, D., Fügenschuh, B., Matenco, L, Schefer, S., Schuster, R., Tischler, M., Ustaszewski, K., 2008. The Alpine-Carpathian-Dinaridic orogenic system: correlation and evolution of tectonic units. Swiss J. Geosci. 101, 139–183.

Seger, M., Alexander, J., 2009. Distribution of Plio-pleistocene and Modern Coarse-grained Deltas South of the Gulf of Corinth, vol. 40. Tectonic Controls and Signatures in Sedimentary Successions (Special Publication 20 of the IAS), Greece, p. 37.

Sharp, I.R., Gawthorpe, R.L., Armstrong, B., Underhill, J.R., 2000. Propagation history and passive rotation of mesoscale normal faults: implications for synrift stratigraphic development. Basin Res. 12 (3–4), 285–305.

Sofilj, J., Živanović, M., 1971. Basic Geological Map of the SFRY, 1:100.000, Sheet Prozor (K-33-12). Federal Geological Institute, Belgrade.

Stojadinović, U., Matenco, L., Andriessen, P.A.M., Toljić, M., Foeken, J.P.T., 2013. The balance between orogenic building and subsequent extension during the Tertiary evolution of the NE Dinarides: constraints from low-temperature thermochronology. Glob. Planet. Change 103, 19–38.

Støren, E.N., Dahl, S.O., Nesje, A., Paasche, Ø., 2010. Identifying the sedimentary imprint of high-frequency Holocene river floods in lake sediments: development and application of a new method. Quat. Sci. Rev. 29, 3021–3033.

Strachan, L.J., Rarity, F., Gawthorpe, R.L., Wilson, P., Sharp, I., Hodgetts, D., 2013. Submarine slope processes in rift-margin basins, Miocene Suez Rift, Egypt. Geol. Soc. Am. Bull. 125 (1–2), 109–127.

Sweet, A. R., Long, D. G. F., Catuneanu, O., 2003. Sequence boundaries in finegrained terrestrial facies: biostratigraphic time control is key to their recognition. In: Geological Association of Canada-Mineralogical Association of Canada joint annual meeting, Vancouver, May 25–28. In Abstracts (vol. 28, p. 165).

Sweet, A.R., Catuneanu, O., Lerbekmo, J.F., 2005. Uncoupling the Position of Sequence-bounding Unconformities from Lithological Criteria in Fluvial Systems. American Association of Petroleum Geologists Annual Convention, pp. 19–22.

Talling, P.J., Masson, D.G., Sumner, E.J., Malgesini, G., 2012. Subaqueous sediment density flows: depositional processes and deposit types. Sedimentology 59 (7), 1937–2003.

Tari, G., Horváth, F., Rumpler, J., 1992. Styles of extension in the Pannonian basin. Tectonophysics 208, 203–219.

Toljić, M., Matenco, L., Ducea, M.N., Stojadinović, U., Milivojević, J., Đerić, N., 2013. The evolution of a key segment in the Europe–Adria collision: the Fruška Gora of northern Serbia. Glob. Planet. Change 103, 39–62.

Tomljenović, B., Csontos, L., 2001. Neogene-quaternary structures in the border zone between Alps, Dinarides and Pannonian Basin (hrvatsko zagorje and Karlovac basins, Croatia). Int. J. Earth Sci. V90, 560–578.

Trudgill, B.D., 2002. Structural controls on drainage development in the Canyonlands grabens of southeast Utah. AAPG Bull. 86 (6), 1095–1112.

Tugend, J., Manatschal, G., Kusznir, N.J., Masini, E., Mohn, G., Thinon, I., 2014. Formation and deformation of hyperextended rift systems: insights from rift domain mapping in the Bay of Biscay-Pyrenees. Tectonics 33, 1239–1276.

Ustaszewski, K., Kounov, A., Schmid, S.M., Schaltegger, U., Krenn, E., Frank, W., Fügenschuh, B., 2010. Evolution of the Adria-Europe plate boundary in the northern Dinarides: from continent-continent collision to back-arc extension. Tectonics 29, TC6017, 6010.1029/2010tc002668.

Ustaszewski, K., Herak, M., Tomljenović, B., Herak, D., Matej, S., 2014. Neotectonics of the Dinarides–Pannonian Basin transition and possible earthquake sources in the Banja Luka epicentral area. J. Geodyn. 82, 52–68.

van Gelder, I.E., Matenco, L., Willingshofer, E., Tomljenović, B., Andriessen, P.A.M., Ducea, M.N., Beniest, A., Gruić, A., 2015. The tectonic evolution of a critical segment of the Dinarides-Alps connection: kinematic and geochronological inferences from the Medvednica Mountains, NE Croatia. Tectonics. http://dx.doi.org/10.1002/2015TC003937.

van Wagoner, J.C., Mitchum, R.M., Campion, K.M., Rahmanian, V.D., 1990. Siliciclastic sequence stratigraphy in well logs, cores, and outcrops. Am. Ass. Pet. Geol. Expl. Ser. 7, 211–240.

van Wijk, J., van Hunen, J., Goes, S., 2008. Small-scale convection during continental rifting: evidence from the Rio Grande rift. Geology 36, 575–578.

Wernicke, B., 1992. Cenozoic extensional tectonics of the U.S. Cordillera. In: B.C., B., Lipman, P.W., Zoback, M.L. (Eds.), The Cordilleran Orogen: Conterminous U.S. Geological Society of America, Boulder, Colorado, pp. 553–581.

Withjack, M.O., Schlische, R.W., Olsen, P.E., 2002. Rift basin structure and its influence on sedimentary systems. In: Renaut, R.W., Ashley, G.M. (Eds.), Sedimentation in Continental Rifts, vol. 73. SEPM Spec. Publ., pp. 57–81

Young, M.J., Gawthorpe, R.L., Sharp, I.R., 2000. Sedimentology and sequence stratigraphy of a transfer zone coarse-grained delta, Miocene Suez Rift, Egypt. Sedimentology 47 (6), 1081–1104.

Zachos, J.C., Pagani, M., Sloan, L., Thomas, E., Billups, K., 2001. Trends, rhythms, and aberrations in global climate 65 Ma to present. Science 292, 686–693.

Ziegler, P.A., Cloetingh, S., 2004. Dynamic processes controlling evolution of rifted basins. Earth Sci. Rev. 64 (1), 1–50.

Živanović, M., Sofilj, J., Milojević, R., 1967. Basic Geological Map of the SFRY, 1:100.000, Sheet Zenica (L-33-144). Federal Geological Institute, Belgrade.

Đerić, N., Gerzina, N., Schmid, S.M., 2007. Age of the Jurassic radiolarian chert formation from the Zlatar mountain (SW Serbia). Ofioliti 32, 101–108.

Đoković, I., 1985. The use of structural analysis in determining the fabric of Paleozoic formations in the Drina - Ivanjica region. Geol. Balk. Poluos 49, 11–160.